AN ABSTRACT OF THE THESIS OF

Harold R. Stroh for the degree of Master of Science in Department of Geology presented on June 28, 1979

Title: Geology of the Clarno Formation in the Vicinity of Stephenson Mountain, Jefferson, Crook and Wheeler Counties, Oregon

Abstract approved: Edward M. Taylor
Dr. E. M. Taylor

The thesis area is located in north-central Oregon approximately 20 km west of the town of Mitchell. The rocks exposed in the area belong to the Clarno Formation.

This study supports the informal reclassification of the Clarno to Group status, composed of an Upper and Lower Clarno Formation. An angular unconformity separates the two Formations. The Lower Clarno Formation is composed of a lower Ross Flat Member dominated by epiclastic sedimentary rocks and an upper Heflin Creek Member composed primarily of pyroxene andesite lavas. The Upper Clarno Formation consists of two conformable units, a lower Quartz-bearing Andesite Unit and an upper Pyroxene Andesite Unit. A thin sequence of rhyolite flows is found near the top of the upper unit. Andesite, dacite and rhyolite rocks intrude the lavas and sediments of the Group.

When plotted on a Peacock diagram the Clarno rocks

are found to be calcic. The chemical variation diagrams and AFM plot of samples, however, follow calc-alkaline trends and compare favorably with rocks considered to be calc-alkaline by others.

Most of the thesis area lies on the southern flank of the east-northeast trending Sutton Mountain Syncline. The northeast trending Mitchell Anticline is found east of the project area and the Lower Clarno rocks follow its' trend. The easterly trending strike-slip Mitchell Fault cuts the northern part of the area. Strata of the area show five kilometers of right-lateral movement along the fault. The angular unconformity separating the formations is found in the eastern part of the area and has been displaced by the Mitchell Fault.

The occurrence of andesitic calc-alkaline volcanism near consuming plate margins is well documented and it is possible that the Clarno rocks may be the surface manifestations of subduction. It would be well to remember, however, that "Not all calc-alkaline rocks of the interior of the western United States are related to subduction" (Robyn, 1977).

Geology of the Clarno Formation in the Vicinity of Stephenson Mountain, Jefferson, Crook and Wheeler Counties, Oregon

by

Harold Raymond Stroh

A THESIS

submitted to

Oregon State University

in partial fulfillment of
the requirements for the
degree of

Master of Science

June 1980

APPROVED:

Edward M. Taylor

Professor of Geology (in charge of major)

Robert S Yeats

Chairman of the Department of Geology

W. H. Beahan

Dean of Graduate School

Date thesis is presented: June 28, 1979

Typed by Karen Genest for: Harold R. Stroh

ACKNOWLEDGMENTS

I want to extend my thanks to Dr. E. M. Taylor for his many helpful suggestions and comments offered during the preparation of this paper. I would also like to thank Dr. Harold Enlows for his help with the petrology and Dr. C. Rosenfeld for critically reading the manuscript.

My special thanks are extended to my wife, Carla, for putting up with me during the preparation of this thesis.

TABLE OF CONTENTS

LIST OF FIGURES

LIST OF FIGURES (continued)

LIST OF TABLES

LIST OF PLATES

Geology of the Clarno Formation in the Vicinity of Stephenson Mountain, Jefferson, Crook and Wheeler Counties, Oregon

INTRODUCTION

Location

The area of this study is within Jefferson, Crook and Wheeler Counties of north central Oregon (Fig. 1). Approximately 87 km^2 were mapped including all or parts of : sections 31-36, T. 11 S., R. 19 E.; section 31, T. 11 S., R. 20 E.; sections 10-14, T. 12 S., R. 18 E.; sections 1-18, T. 12 S., R. 19 E.; and sections 6, 7, and 13, T. 12 S., R. 20 E. The project area is shown on the Stephenson Mountain and Opal Mountain Quadrangles and its southern three-fourths lies within the northern part of the Ochoco National Forest.

Physiography and Climate

The project area lies within the maturely dissected volcanic-volcaniclastic terrain of the Ochoco Mountains. Topography consists of deep, steep-sided valleys with prominent ridge lines, gentle slopes approximating the present dip of inclined strata, flat topped mesas composed of rhyolite flows and small hummocky hills of slumped debris.

Total relief in the area is about 945 m with elevation ranges from 1,785 m in the rhyolitic terrain in the southwest part of the area to about 840 m along Bear

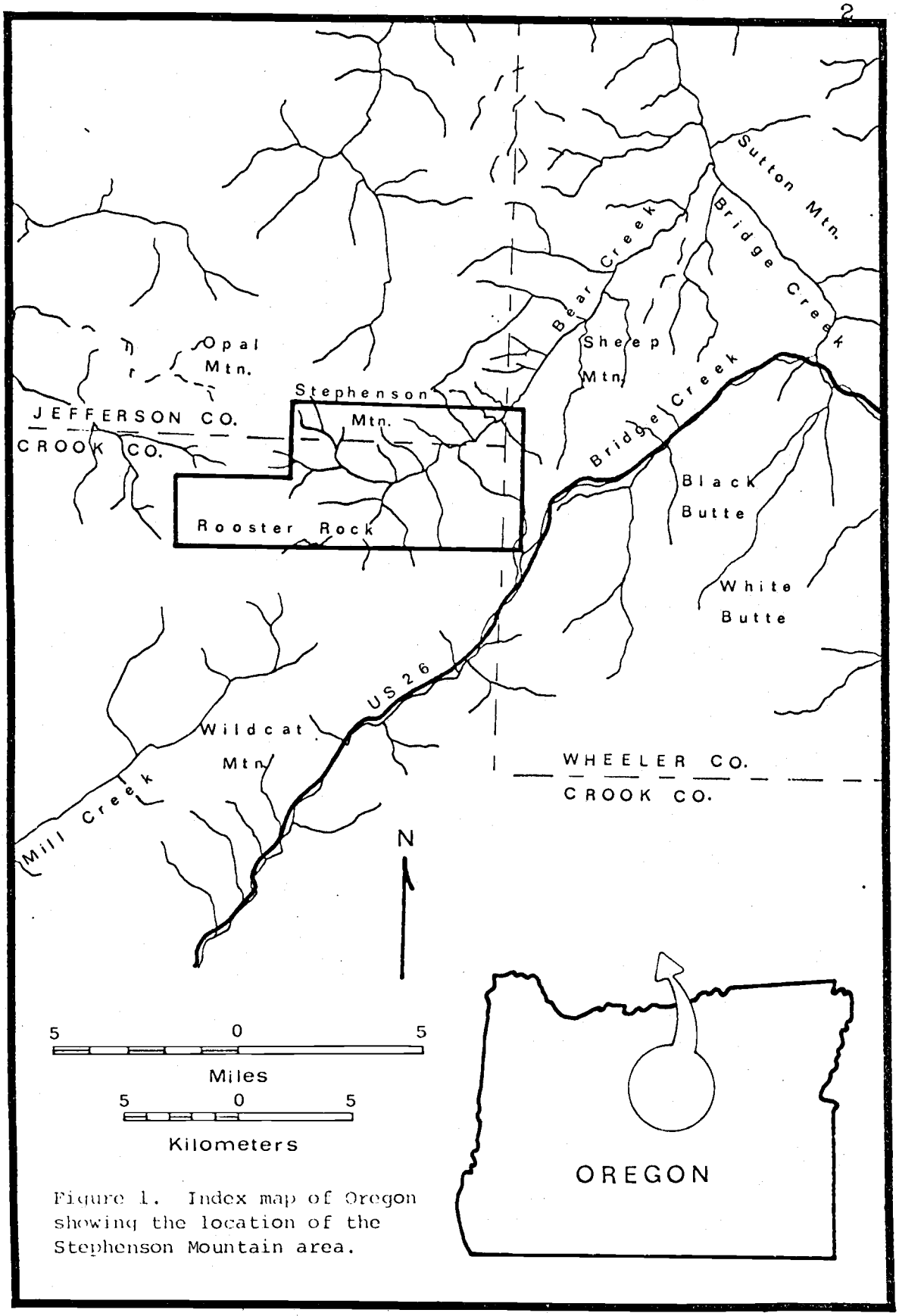

Figure 1. Index map of Oregon showing the location of the Stephenson Mountain area.

Creek in the northwest. Typical slopes are from 200 to 300 meters per kilometer.

The dendritic drainage pattern within the area is dominated by Bear Creek which empties into Bridge Creek several miles to the northeast. A small part of the northwest corner of the area is drained to the west by Trout Creek and its tributaries.

The eastern margin of the project area lies within the rainshadow of the Ochoco Mountains. Vegetation consists mostly of juniper, sagebrush and range grass typical of the dryer parts of eastern Oregon. To the west and south, approaching the crest of the Ochoco Mountains, precipitation is more abundant. Sagebrush and juniper of the lowlands rapidly gives way to dense forests of second growth pine and fir.

Accessibility and Exposure

The project area can be reached from U.S. Highway 26 which is a major east-west thoroughfare through this part of Oregon. Light-duty forest service roads which emanate from the highway provide access to the western and southern parts of the area. The remaining area is accessable by ranch roads east of Ochoco Summit. Many of the roads in the area have fallen into disuse and are traversable in places only by four-wheel-drive vehicles. During years of heavy snowfall many of the roads are

blocked until the later weeks of April.

Exposures in the area are a function of the abundance of vegetation. In the dryer northeastern one-third of the area vegetation is sparse and exposures are excellent. In the higher areas, to the south and west where thick forest soils have developed, mapping was accomplished mostly with the aid of float.

Purpose and Methods of Investigation

The main purpose of this investigation was to construct a geologic map and to describe the mineralogical and chemical composition of the rock units of the Stephenson Mountain area as an aid in locating the Mitchell Fault. Little work has been done on these rocks as far as the structural relations are concerned. Owen (1977) accurately determined the location of the Mitchell Fault further east where Clarno volcaniclastics have been juxtaposed against Clarno lavas. He also inferred its approximate location within the northeastern part of this study area. Recognition of the fault west of this point has been hampered by poor exposures and the apparent lack of megascopic variation between the volcanic units. Similarly, the existence and location of an angular unconformity presumed to exist between the Upper and Lower Clarno (Oles and Enlows, 1971) has been in doubt. It is hoped that this study will contribute to a better

understanding of the Clarno Formation and clarify the structural and stratigraphic relationships of the area.

A total of ten weeks was spent in geologic mapping during the spring and fall of 1978. An additional two week period was spent in the field during March 1979 working on particular problems. Field data were plotted directly on 7.5-minute U.S. Geological Survey Opal Mountain and Stephenson Mountain Quadrangles. Aerial photographs of approximately 1:62,500 scales were used as an aid to the mapping. The colors of all samples, fresh and altered, were named in accordance with the Rock Color Chart published by the Geological Society of America (Goddard 1970). Attitudes of beds were measured with a brunton compass and the thicknesses of units were calculated from mapped elevations and distances.

Approximately 200 samples were collected. Of these, the less altered specimens were examined in further detail in the laboratory. Seventy thin sections were examined to determine the microscopic characteristics of the different lithologic units. Modal analysis of phenocrystic constituents were performed using 750 counts per section. Compositions of well developed, unaltered Plagioclase crystals were determined by the Combined Albite-Carlsbad method of Kohler (1923; in Tobi, 1963). The statistical method of Michael-Levy was employed to determine the composition of less suitable crystals.

Whole rock chemical analysis was performed in 10 samples considered to be representative of the mapped units. Weight percentages of FeO (total iron), TiO_2, CaO, K_2O and Al_2O_3 were determined by X-ray fluorescence spectrometry, Na_2O and MgO were determined by atomic absorption spectrometry and SiO_2 was determined by both X-ray fluorescence and a silicomolybdate colorimetric method. The analyses were performed on roasted rock powders and are water free. The analytical runs were performed by Ruth L. Lightfoot and Dr. E. M. Taylor, Department of Geology, Oregon State University.

Igneous rock nomenclature was based on weight percent increments of SiO_2. The subdivisions used are those proposed by Taylor (1978). Rocks with an SiO_2 content between 48 and 53 percent are classified as basalts, between 53 and 58 percent as basaltic andesites, between 58 and 63 percent as andesites, between 63 and 68 percent as dacites, and more than 68 percent as rhyodacite. Rhyolites are defined as those rocks containing greater than 73 percent SiO_2 and greater than 4 percent K_2O.

The volcaniclastic rocks are named according to the classification of Fisher (1961).

Regional Geology

The project area contains sections of the Upper and Lower Clarno Formations of the Clarno Group. These

formations are the lower units in a succession of Cenozoic volcanic and volcaniclastic rocks found in central and eastern Oregon. The position of the Formations in the regional stratigraphic section is shown in Figure 2. Potassium - argon dates provided by Enlows and Parker (1972) indicate that Clarno activity spanned the time period from about 46 to 29 million years before present.

Regionally, the Clarno Group is composed of lavas, tuffs, mudflow deposits, epiclastic sediments, and a variety of intrusives including dikes, sills and plugs. The lavas and intrusives range in composition from basaltic to rhyolitic and as a group are calc-alkaline to calcic.

Within the project area andesitic lavas make up the bulk of the exposures. Along the eastern boundary, however, is the Ross Flat Member (Owen, 1977) of the Lower Clarno Formation which is dominated by epiclastic sandstone and siltstones interbedded with minor lavas and mudflows. Near the top of this unit a cliff-forming welded tuff serves as a valuable marker horizon. Several dikes and plug-like intrusions are present and range in composition from andesite to rhyolite.

Several folds are found in this region. The largest of these is the Blue Mountains Anticlinorium which can be traced from the vicinity of Prineville for about 320 km to the area of Wallowa Mountains of northeastern Oregon

AGE		FORMATION	LITHOLOGY
QUARTERNARY	PLEISTOCENE	QUATERNARY DEPOSITS	ALLUVIUM
TERTIARY	PLIOCENE	DESCHUTES AND RATTLESNAKE	FLUVIAL SANDSTONE SILTSTONES, TUFFS MUDFLOWS, BASALT CONGLOMERATES ANDESITE IGNIMBRITES IGNIMBRITE FANGLOMERATE
	UPPER MIOCENE	MASCALL COLUMBIA RIVER GROUP PICTURE GORGE BASALT	FLUVIAL SANDSTONE CONGLOMERATE, ASH IGNIMBRITE, TUFF THOLEIITIC BASALT
	LOWER MIOCENE TO MIDDLE OLIGOCENE	JOHN DAY	TUFF, IGNIMBRITE RHYOLITE ALKALI BASALT TRACHYANDESITE
	LOWER OLIGOCENE TO MIDDLE EOCENE	CLARNO	BASALT, ANDESITE DACITE, MUDFLOW RHYODACITE, TUFF INTRUSIVE ROCKS
CRETACEOUS	ALBIAN TO CENOMANIAN	HUDSPETH GABLE CREEK	MARINE MUDSTONE GRAYWACKE CONGLOMERATE
PERMIAN		METASEDIMENTS	GLAUCOPHANE-LAWSONITE SCHIST, PHYLLITE

Figure 2. Generalized stratigraphic column for north-central Oregon. After Rogers and Novitsky-Evans (1977).

(Fisher, 1967). The other broad warps in the area include the east-northeast trending Sutton Mountain Syncline and the northeast trending Mitchell Anticline. The axis of the syncline is present in the northwestern part of the area and most of the rocks in the area are on its southern limb. The anticline is found several kilometers east of the project area. The stresses which produced it have effected similar deformation to the Lower Clarno rocks of the study area.

Several east-west trending faults occur in the area. The majority of these are probably related to the east-west, right-lateral, strike slip Mitchell Fault which transects the region. The Mitchell Fault has a displacement of about 5 km and can be traced to the area of Mitchell several kilometers to the east. Its extent and location west of the study area is unknown.

Previous Work

The Clarno Formation was named by Merriam (1901) for a series of tuffs, mudflows and andesitic and rhyolitic lavas underlying the John Day Formation. Type Clarno is exposed at the site of the Clarno Ferry on the John Day River 50 km north of the study area. Knowlton (1902) published a study of the Tertiary flora of the Clarno and assigned an Eocene age to the Formation. Based on similar fossils Chaney (1952) considered the

formation to be Middle and Upper Eocene. These age determinations are supported by Scott (1954) in his descriptions of a "nutbed" locality near Clarno Bridge. Additional floral studies have been recently completed by Gregory (1970) and McKee (1970).

Faunal assemblages from the Clarno Formation have been described by Stirton (1944) and Hansen (1973). Important unpublished work has been done by the late amateur paleontologist, Lon Handcock of Portland. A large collection of the fossils he recovered from a locality near Clarno Bridge has been assembled by A. Shotwell and now resides at the University of Oregon Museum of Natural History.

Calkins, (1902) who had accompanied Merriam on early expeditions into central Oregon, published the first petrographic study of the formation. Waters, et al., (1951) discussed the petrology of the Clarno and its relation to the quicksilver deposits of the Horse Heaven Mining District. Swanson and Robinson (1968) assigned a porphyritic rhyolite flow within the mining district to the Clarno on the basis of a 41.0±1.2 m.y. age date obtained from the flow. These rocks are too old to be placed within the John Day Formation, but fall well within the recognized age of the Clarno.

Wilkinson and Oles (1971) were the first to publish a map delineating the location of the Mitchell Fault

east of the project area. Oles and Enlows (1971) informally reclassified the Clarno as a group, divided into an Upper and Lower Clarno Formation.

Two Upper Clarno rocks from the vicinity of Mitchell, Oregon, have been dated by Everden et al., (1964) as Early Oligocene. Everden and James (1965) produced a potassium-argon date of 34.0 m.y. from the Clarno nutbeds. More recent dating by Enlows and Parker (1972) indicates that Clarno igneous activity spanned the time interval from Late Eocene to Middle Oligocene. The following year Enlows and Oles (1973) summarized the stratigraphy and geochronology of the Clarno in the Mitchell area.

Two theses dealing with parts of the project area have been submitted by Masters candidates of Oregon State University (Lukanuski, 1963; Owen, 1977). A suitable base map was not available to Lukanuski, hence his portrayal of the stratigraphic relationships of the volcanic units lacked sufficient detail to support meaningful interpretations. Owen mapped the lithologic units cut by the Mitchell Fault in the easternmost part of the project area.

Published geologic maps of the area include a 1:250000 reconnaissance map by Swanson (1969) and an updated 1:125000 version by Robinson (1976).

STRATIGRAPHY

Clarno Group: Introduction

The stratigraphic section of the rocks in the project area is divided into two major units by an angular unconformity. This unconformity is believed to represent the same hiatus recognized in the Mitchell area to the east by Oles and Enlows (1971). This author will follow the example of Oles and Enlows (1971) and informally refer to the Clarno as a Group, composed of an Upper and Lower Clarno Formation.

The Clarno Group has unconformable contacts with the underlying Cretaceous Formations (Oles and Enlows, 1971; Owen, 1977) and the overlying Tertiary John Day Formation (Peck, 1964; Huggins, 1978). Neither of these contacts is exposed in the project area. The unconformable contact separating the Upper and Lower Clarno Formations is discussed in this report under the heading "Structure". This unconformity is well exposed in the Mitchell Quadrangle (Oles and Enlows, 1971), and has been identified north of the Mitchell Fault five kilometers northeast of the study area by Taylor (1979 personal communication). The thickness of the Clarno Group within the project area is difficult to estimate because of faulting and multiple faulting but is probably within 200 m of 2,500 m. Chemical analyses of rocks from the different units

of the Group are presented in Appendix A.

Lower Clarno Formation: Introduction

In the Mitchell Quadrangle where the Lower Clarno Formation was first informally defined it is made up of volcanic breccias, andesite flows and varicolored tuffaceous sediments (Oles and Enlows, 1971). In the area of this study the Lower Clarno is made up of andesite flows, mudflows, epiclastic sedimentary rocks and a widespread Clarno-age ignimbrite. Within the study area the Lower Clarno has a maximum thickness of about 950 m and, as mentioned previously, has unconformable upper and lower contacts.

Owen (1977) mapped some of these Lower Clarno rocks and their extensions to the east and grouped the rocks into two members. The older of the two members is composed predominately of epiclastic sedimentary rocks but also contains mudflows, an ignimbrite, and minor andesitic lavas. Owen informally named this group of rocks the Ross Flat Member and his usage will be followed in this study. The younger of the two members of the Lower Clarno as defined by Owen (1977) is composed of andesitic lavas and minor mudflows and is informally referred to as the Stephenson Mountain Member. The results of this study suggest that this member is not nearly as widespread as indicated by Owen and is not found on Stephenson

Mountain. Therefore, to avoid confusion, the sequence of lavas and mudflows conformably overlying the Ross Flat Member in this region is informally renamed the Heflin Creek Member. The name is derived from a creek along which the member is exposed. The contact between the Ross Flat and Heflin Creek Member is gradational. Some andesitic lavas extend into the Ross Flat Member and a few mudflows can be found in the lower part of the Heflin Creek Member. For convenience the boundary between the two members is placed at the top of a well exposed ignimbrite which occurs near the base of the andesitic lavas.

Ross Flat Member

The Ross Flat Member is the oldest unit of the Lower Clarno Formation exposed in the project area. The member covers about 5.5 km^2 and makes up 6 percent of the rocks in the study area. In the Stephenson Mountain area the member has a thickness of about 500 m.

Regionally the member is composed of epiclastic and tuffaceous sandstones, siltstones and claystones with minor interbedded units of pebbly sandstone, mudstone, ignimbrite and lava. In the surrounding areas the member generally makes up the middle of the Lower Clarno Formation with a thick sequence of Clarno andesites above and below.

In this study the limits of the member are those informally proposed by Owen (1977). The top of the member is marked by a widespread ignimbrite. In the northeastern parts of the study area the Ross Flat Member is conformably overlain by the Heflin Creek Member of the Lower Clarno Formation. In the southeastern parts of the area the Ross Flat Member is unconformably overlain by andesitic lavas of the Upper Clarno Formation. The lower contact of the Ross Flat Member is not exposed in the project area. Owen(1977) has mapped the basal contact of the member three kilometers to the east where it rests unconformably on Cretaceous sediments. For the purposes of discussion the Ross Flat Member is divided into three types of deposits: 1) Epiclastic sedimentary rocks, 2) Mudflow deposits and 3) Ignimbrite.

Epiclastic Sedimentary Rocks

The epiclastic sedimentary rocks of the Ross Flat Member are exposed along the eastern margin of the project area. The rocks making up these deposits are less resistant to erosion than the overlying lavas, hence they occupy the topographically low-lying regions. Steep slopes develop where these rocks are protected by overlying lavas.

The strata making up these deposits are broad sheet-like units which are continuous over wide areas. The

beds shown in Figure 3 can be traced for a distance of .6 km. Over this interval the individual strata are nearly constant in thickness. Sedimentary structures identified in these rocks include repetitive normal graded bedding and small scale symmetrical ripple marks. Poorly developed low-angle cross-bedding also occurs but displays no preferred orientation. Carbonized fragments of wood, oriented parallel to the bedding planes are found in the finer grained sandstones and siltstones. These fine-grained units also contain casts of Equisetum stems in growth position.

The particles making up these rocks generally vary in size from silt to very coarse sand. Occasional thin lenses of small to medium size pebbles do occur but are relatively rare. Framework grains in these coarser units are often subangular to subrounded giving the rock a microbreccia texture. Sorting is poor in all but the very fine grained units. Texturally and compositionally the rocks are immature. Fresh exposures of the rock vary from pale olive (10Y 6/2) to pale greenish yellow (10Y 8/2). Weathered exposures are various hues of green and yellow.

As indicated previously these strata maintain a fairly constant thickness over broad areas and are often thinly bedded. It is also of note that no marine fossils have been recovered from these rocks. Taken together

Figure 3. Photograph of outcrops of epiclastic sedimentary rock of the Ross Flat Member, Lower Clarno Formation. The bed in the center of the field of view is .9 m thick. (NE$\frac{1}{4}$, Sec. 6, T. 12 S., R. 20 E.)

these facts suggest that these rocks were deposited in a lacustrine environment. Most of the strata are poorly sorted and, based on their make-up, were probably derived from andesitic volcanic rocks which presumably bordered the basin of deposition. A progressive fining of the units to the northwest suggests that the basin became deeper in that direction. This is also suggested by an increase in the occurrence of mudflows and plant fossils to the southeast.

In thin section these rocks are made up of monomineralic grains, lithic fragments and fine grained matrix. The abundance of matrix increases from about 15 volume percent in the well sorted fine-grained units to about 50 volume percent in the more poorly sorted units. The matrix is made up of clay, altered fragments of the monomineralic grains and devitrified glass shards. The products of devitrification have not been positively identified but probably include quartz, feldspar, and smectite clay minerals.

The monomineralic grains include plagioclase, quartz, orthopyroxene, clinopyroxene, and hornblende. Plagioclase commonly makes up 40 volume percent of the rock in thinsection. The plagioclase has a maximum size of 0.9 mm in diameter and shows only slight alteration. Occasionally, calcite can be seen as a replacement along

fractures in the mineral. Quartz in these sediments is present only in the better sorted, finer grained units. Although angular fragments do occur, most of the quartz is rounded to subrounded. It ranges in size up to 2.0 mm and makes up a maximum of 8 volume percent of the rock. Many of the quartz grains display regularly spaced sets of fractures which intersect at right angles. This characteristic is not common in quartz of volcanic rocks and suggests that the quartz may have been derived from the underlying Cretaceous Formations. The size, shape and anomalous abundance of the grains supports this possibility.

Ferromagnesian minerals generally make up from 1 to 2 volume percent of the rock. The grains are fragmented and are usually less than 0.5 mm in length. Although alteration is more severe in the hornblende, all species have been at least partially replaced by hematite and chlorite.

The lithic constituents making up the sediments are, in descending order of abundance, andesite, chert, basalt, and pumice. The andesite fragments occur in all of the sediments examined. In the coarser grained sandstones andesitic fragments make up a maximum of 17 volume percent of the rock. The fragments occur as porphyritic rounded to subrounded grains up to 2.0 mm in diameter and display many of the characteristics of the andesite

flow rocks of the area. Chert, which makes up 5 to 10 volume percent of the rock, displays the same mosaic texture seen in the devitrified volcanic glass. Like the quartz it is fairly well rounded and was probably derived from the underlying Cretaceous formations. Basaltic fragments make up from 5 to 10 volume percent of the rock as subangular to subrounded grains which range in size from 0.3 to 1.2 mm. The basalt is commonly vesicular, has a felted groundmass and is palagonitized. Pumice is the least abundant lithic constituent in these rocks. It makes up to 4 volume percent of the thin-sections and occurs as elongated flattened grains. The pumice is completely devitrified to fine-grained quartz and feldspar.

Mudflow Deposits

Volcanic mudflows are present at several locations in the eastern part of the project area. The deposits have not been mapped as a separate unit of the Ross Flat Member because of their limited distribution. Good exposures can be seen along the Stephenson Ranch - Heflin Creek road and on the eastern slopes of the ridge dividing the Dodds and Heflin Creek drainages. The mudflows are too limited in number and extent to influence the topography of the area; they are confined with the sedimentary rocks to the lower slopes and valleys.

Outcrops of the mudflows consist of subrounded to rounded, coarse sand to boulder sized clasts of andesite in a matrix of the same composition. The outcrops weather to various hues of green and gray and often contain randomly oriented fragments of silicified wood. Generally the deposits are in matrix support and are extremely poorly sorted. Exceptions to this poor sorting were observed in a few outcrops which appear to contain concentrations of larger fragments in their upper sections. According to Waldron (1966; in Schmincke, 1967) reverse grading in mudflows may be due to the "Selective removal of larger fragments that projected upward into higher velocity zones during flow." Other explanations for the reverse grading in mudflows (Fisher and Matlinson, 1968) are based on the experimental work of Bagnold (1954) which demonstrates that in grain flows the larger particles migrate away from the zone of maximum shear strain. Why this happens is imperfectly understood but is probably related to the "Mangus effect" which Bhattachavji (1967) used to explain the size distribution of crystals in the feeder dike of the Muskox Intrusion in Canada.

Most of the clasts of andesite seen in these mudflows are similar in handsample to the andesite which makes up the Heflin Creek Member of the Lower Clarno Formation. One type of clast, which is not represented

by the Clarno lavas of the study area, is made up of porphyritic hornblende andesite. This rock type makes up from 5 to 45 percent of the mudflow clasts of some exposures. Fresh surfaces of the rock are a grayish orange pink (5YR 7/2) and weathered exposures are typically yellowish brown (10YR 5/4). Plagioclase and hornblende are the only phenocrysts visible in handsamples.

Phenocrysts present in thinsection include plagioclase, hornblende and magnetite. The plagioclase occurs as subhedral elongate tablets up to 1.0 mm in length. The crystals are compositionally andesine (An_{38}-An_{40}) and make up about 23 volume percent of the rock. Most of the plagioclase phenocrysts in the rock display well developed oscillatory zoning. Hornblende phenocrysts make up about 7 volume percent of the rock as subhedral laths with a maximum size of about 5.0 mm. Magnetite phenocrysts account for about 2 volume percent of the rock as anhedral crystals up to 0.3 mm in diameter. The rock has a poorly developed pilotaxitic texture with a groundmass made up of plagioclase, clinopyroxene, magnetite and glass.

Ignimbrite

A Clarno age ignimbrite, well exposed in the eastern part of the project area, is the youngest unit of the Ross Flat Member. A chemical analysis by Oles and Enlows

(1971) shows that the ignimbrite is a rhyolite with a high amount of potassium. The ignimbrite crops out along Heflin Creek and is exposed from there northward for a distance of 2 km. South of Heflin Creek the unit can be traced for a distance of 1.6 km to the SW$\frac{1}{4}$, Sec. 13, T. 12 S., R. 19 E., where it is buried by Upper Clarno lavas. The ignimbrite is also exposed on the ridge north of old Stephenson Ranch and east of the study area where it caps numerous small buttes (Owen, 1977).

The thickness of the ignimbrite varies considerably. Along Heflin Creek its contacts are obscured by talus but exposures suggest that it is at least 35 m thick. In the remainder of the project area it never exceeds 15 m in exposed thickness. Fresh exposures of the rock are pale greenish yellow (10Y 8/2) and weathered surfaces vary from pale olive (10Y 6/2) to greyish green (5G 5/2).

The ignimbrite often forms cliffs which display crude columnar jointing (Fig. 4). The columns are up to .5 m in width and 10 m in length. They are best developed in the lower central part of the unit which may belong to the lower welded zone of the ignimbrite sequence described by Ross and Smith (1961). The other zones they discussed were not found.

The lower central part of the ignimbrite is composed of lithic fragments (15-20%) and sanidine crystals

Figure 4. Photograph of an outcrop of ignimbrite showing columnar jointing. The columns near the center of the field of view are .3 m wide. (NE¼, Sec. 12, T. 12 S., R. 19 E.)

(5-10%) in a matrix of devitrified glass with a well developed eutaxitic texture (Fig. 5). The products of devitrification have not been positively identified but probably include quartz and feldspar. Sanidine crystals in the rock are always at least partly altered to calcite. The rock types making up the lithic fragment population include andesite (50-70%), sediments (15-25%) and flattened pumice (10-20%). Nearer the base of the ignimbrite the abundance of lithic fragments making up the rock increases to about 35 volume percent. This increase is made up principally of a greater number of sedimentary rock fragments. These fragments were probably derived from the underlying epiclastic sediments of the Ross Flat Member.

Heflin Creek Member

The Heflin Creek Member of the Lower Clarno Formation is made up of the oldest series of extrusive volcanic rocks in the project area. The member is less abundant than most other lava units of the Clarno Group. It covers an area of about 3 km^2 and has a maximum thickness in the project area of 450 m. Exposures of this member occupy a 4 km long northeast-trending belt and make up about 4 percent of the project area.

Lavas of the Heflin Creek Member form broad sheet-like deposits which are exposed in prominent southeast

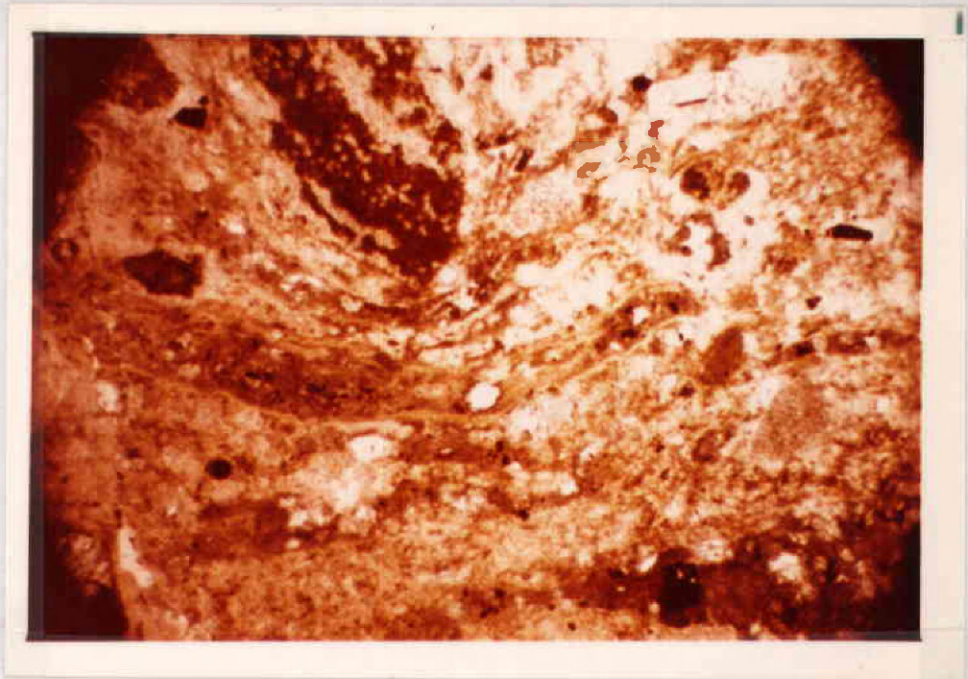

Figure 5. Photomicrograph of Ross Flat Member ignimbrite showing well developed eutaxitic texture. Plane polarized light; field width is approximately 7 mm. (Sample HS78315 from NE½, Sec. 12, T. 12 S., R. 19 E.)

facing cuestas. These cuestas are particularly well developed in the Heflin Creek drainage in Sec. 12, T. 12 S., R. 19 E. Contacts between individual flows of the member are not well exposed. Flow breccias and zones of weathered material are absent. Occasionally contacts can be determined based on changes in color or jointing characteristics of adjacent flows. On the basis of these contacts the flows were estimated to vary in thickness from 3 to 25 m. Platy jointing is well developed in these lavas. It is spaced at 1 to 5 cm intervals and the surfaces of the plates are slightly curved. In a general way the strike of the jointing tends to mimic the strike of the lavas. The dip suggested by the joints, however, often deviates from the true dip by as much as 35 degrees. The lavas are generally not vesicular and only rarely display flow structures visible in handsample. Phenocrysts identified in hand-sample are pyroxene and plagioclase. Surfaces of the rock are often pock-marked due to the weathering out of these minerals. This characteristic was not observed in the overlying quartz-bearing andesites of the Upper Clarno. Colors of the fresh rock approximate a medium bluish grey (5B 5/1). Weathered surfaces are variable but include pale yellowish brown (10YR 6/2) and dark yellowish brown (10YR 4/2).

All of the Heflin Creek Member andesites examined in thinsection display a fairly well developed pilotaxitic texture. Intergranular texture is also present and is best developed in the rocks with the greater amounts of groundmass pyroxene and magnetite. Glomeroporphyritic texture is also common (Fig. 6). Curiously, the pyroxene in the glomerocrysts frequently appears in greater relative abundance than in the rest of the rock.

All of the Heflin Creek Member andesites examined in thinsection are porphyritic with plagioclase, orthopyroxene, and clinopyroxene. In addition biotite phenocrysts are occasionally present and magnetite is of large enough size in a few of the andesites to be termed a phenocryst. A volumetric modal analysis of phenocrysts present in thinsections representative of the unit is shown in Table 1.

The plagioclase phenocrysts make up a maximum of 15.5 volume percent of the rock in thinsection and average 11 percent. The crystals occur as euhedral to subhedral tablets up to 1.8 mm in length. Occasionally the plagioclase grains have rounded corners. Presumably this is a result of late stage resorption. The plagioclase is labradorite, ranging in anorthite content from 52 to 63 percent.

Figure 6. Photomicrograph showing glomeroporphyritic texture of Heflin Creek Member andesite. Cross polarized light; field width is approximately 7 mm. (Sample HS7823 from SE$\frac{1}{4}$, SE$\frac{1}{4}$, Sec. 1, T. 12 S., R. 19 E.)

Table 1. Volumetric modes of phenocryst phases of selected Heflin Creek Member Andesites, Lower Clarno Formation.

Sample	HS7899	HS7823	HS7851	HS7822	HS7871
Labradorite	15.0%	8.5%	6.1%	4.2%	15.5%
Clinopyroxene	4.7%	4.5%	1.2%	3.2%	3.5%
Orthopyroxene	.6%	2.5%	.2%	.2%	1.0%
Magnetite	-	-	tr.	-	-

(tr.= less than .2%)

Sample Locations:

HS7899 Elevation 3,520 ft.; SW¼, NW¼, Sec. 1, T. 12 S., R. 19 E.

HS7823 Elevation 4,280 ft.; SE¼, SE¼, Sec. 1, T. 12 S., R. 19 E.

HS7851 Elevation 4,080 ft.; NW¼, NE¼, Sec. 12, T. 12 S., R. 19 E.

HS7822 Elevation 3,520 ft.; NW¼, SE¼, Sec. 1, T. 12 S., R. 19 E.

HS7871 Elevation 3,330 ft.; SE¼, SE¼, Sec. 36, T. 11 S., R. 20 E.

Several types of zoning are displayed by the plagioclase of these andesites. Although normal zoning is the most common, reverse and well developed oscillatory varieties (Fig. 7) are also present. Vance (1962) explains oscillatory zoning in terms of the diffusion-supersaturation theory of Hills (1936; in Vance, 1962). He states (p. 751):

> "The mechanism operates as follows: (1) diffusion of anorthitic material brings about supersaturation of the melt immediately adjacent to the crystal; (2) when a certain value of supersaturation is reached, crystallization of a small normal zone takes place, impoverishing the adjacent melt in its anorthitic component; (3) diffusion of the new anorthitic material to the crystal fails to keep pace with crystallization, which consequently slows and then ceases; (4) the sequence is repeated."

Hence, there would be developed a normal stepwise progression from a more calcic interior to a more sodic margin. Taylor (1979, personal communication) has suggested that the oscillatory zoning displayed by the plagioclase of these rocks is a result of pressure fluctuations accompanying the eruptions which vent these magmas to the surface. A decrease in confining pressure in the system $NaAlSi_3O_8$-$CaAl_2Si_2O_8$-H_2O was shown by Bowen (1913) to cause an increase in the liquidus temperature of the magma resulting in the crystallization of a less-calcic, more-sodic feldspar. A series of such pressure fluctuations would produce a zoned feldspar with a calcic core and a sodic margin with local rever-

Figure 7. Photomicrograph of Heflin Creek Member andesite showing a plagioclase crystal with well developed oscillatory zoning. Plane polarized light; field width is approximately 7 mm. (Sample HS7822 from SE¼, Sec. 1, T. 12 S., R. 19 E.)

sals in adjoining zones.

Albite is the most common type of twinning seen in the plagioclase phenocrysts of these andesites. Carlsbad and pericline varieties are also present but are usually not well developed.

Plagioclase alters to a greater variety of minerals than the other phases in these andesites. Alteration products identified include chlorite, calcite, smectite clays, and a zeolite, probably heulandite.

Clinopyroxene is the predominate pyroxene phenocryst in the lavas of the Heflin Creek Member. It occurs as neutral colored, euhedral to anhedral tabular crystals up to 1.5 mm in length and is often twinned. On the basis of the optic sign and 2V of the pyroxene it is thought to be augite. It makes up a maximum of 5 volume percent of these rocks and averages 3.9 percent. Alteration products of the augite are magnetite and chlorite. The magnetite occasionally forms nearly complete pseudomorphs after a parent augite crystal.

Orthopyroxene phenocrysts in lavas of the Heflin Creek Member vary in color from neutral to pale pink and often show a faint flesh-colored pleochroism. On the basis of the optic sign and 2V the pyroxene is thought to be hypersthene. Crystals of the hypersthene are euhedral to subhedral, vary in length up to 2.0 mm and are more elongate than the augite. The hypersthene

makes up a maximum of 2.5 volume percent of the rock in thinsection and averages 0.7 percent. Alteration products are the same as those developed in the augite, namely chlorite and magnetite.

Magnetite is present as a phenocryst phase in a few of these andesites. It occurs in trace amounts as anhedral crystals up to 0.3 mm in diameter and is occasionally altered to hematite.

Heflin Creek Member andesites from the NE$\frac{1}{4}$, Sec. 1, T. 12 S., R. 19 E. were found to contain phenocrysts of biotite. The biotite is present as subhedral to anhedral crystals which vary in length up to 0.8 mm. The crystals make up an average of 5.6 volume percent of the rock and are almost entirely altered (Fig. 8). The alteration product is pleochroic in shades of pale green and is strongly birefringent. It is optically negative, has a 2V of about 20° and is length slow. Dr. Harold Enlows of Oregon State University has tentatively identified the mineral as green biotite. It is an alteration product intermediate between fresh biotite and biotite altered to chlorite.

Groundmass phases present in the Heflin Creek Member andesites include plagioclase, clinopyroxene, orthopyroxene, magnetite and biotite. These minerals generally show alteration similar to that displayed by the phenocrysts of the andesites. The plagioclase is

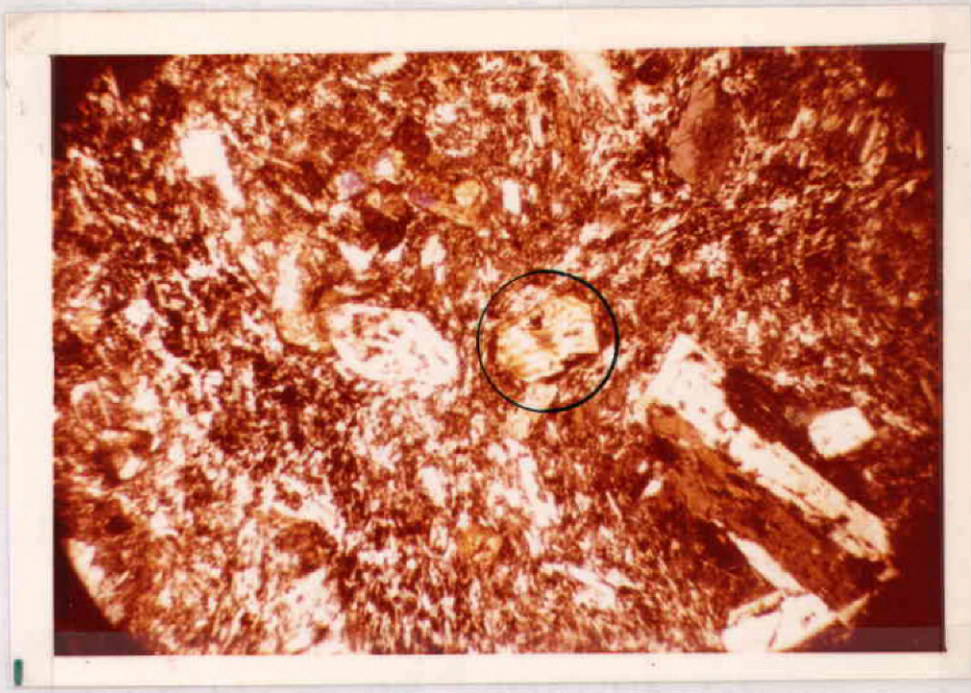

Figure 8. Photomicrograph of Heflin Creek Member andesite showing altered biotite crystals (circled). Cross polarized light; field width is approximately 7 mm. (Sample HS7899 from NE¼, Sec. 1, T. 12 S., R. 19 E.)

present as euhedral to subhedral laths with a maximum size of 0.2 mm. The crystals vary from calcic andesine to sodic labradorite (An_{45}-An_{54}) and make up from about 45 to 70 volume percent of the rock. The groundmass pyroxenes were too small to be positively identified but are probably augite and hypersthene. Together they make up from 4 to 22 volume percent of the rock as anhedral to subhedral crystals. Magnetite is present as euhedral to anhedral grains and makes up a maximum of 3 volume percent of the rock. Groundmass biotite is restricted to those andesites containing biotite as a phenocryst. It occurs as anhedral shreds and flakes and makes up less than 1.0 volume percent of the rock.

Upper Clarno Formation: Introduction

In the Mitchell Quadrangle where the Upper Clarno Formation was first informally defined it is made up of mudflows, tuffaceous sediments, andesite flows and vent agglomerate (Oles and Enlows, 1971). In the area of this study the Upper Clarno is made up, almost entirely, of lava flows. Deposits of epiclastic sediments and mudflows are of very limited distribution. As a result, these deposits are not differentiated on Plate 1 and do not warrant separate discussion as individually mapped units of the Upper Clarno Formation. Where these deposits are present they are similar to their counterparts

in the Ross Flat Member of the Lower Clarno Formation. The Upper Clarno Formation has angularly unconformable upper and lower contacts.

Within the project area the Upper Clarno has a thickness of about 1,530 m and can be divided into two major mapable units. The older unit consists of a series of andesites which contains megascopically identifiable quartz phenocrysts and is referred to as the Quartz-bearing Andesite Unit. These andesites are overlain by the second major unit which contains no megascopic quartz and is referred to as the Pyroxene Andesite Unit. The boundary between the two units is gradational and angularly conformable. Pyroxene andesites, identical to the lavas of Pyroxene Andesite Unit occur randomly throughout the stratigraphic section of the Quartz-bearing Andesite Unit. These pyroxene andesites make up from 40 to 50 percent of the Quartz-bearing Andesite Unit and have been included in the unit in order to simplify field mapping and cartography. For convenience the boundary between the two units is placed at the top of the uppermost andesite flow which contains megascopically recognizable quartz phenocrysts. The pyroxene andesites included in the Quartz-bearing Andesite Unit are discussed along with andesites of the Pyroxene Andesite Unit.

Near the top of the Pyroxene Andesite Unit a series

of rhyolite flows are present. On a small scale the rhyolites are erosionally unconformable to the andesites of the Upper Clarno. Exposures suggest that the rhyolites filled canyons eroded into the Upper Clarno rocks. On a larger scale the rhyolites are conformable to the andesites as suggested by the similar attitudes displayed by both units. Although the rhyolites occur within the stratigraphic section of the Pyroxene-bearing Andesite Unit, they are discussed separately.

Quartz-bearing Andesite Unit

The Quartz-bearing Andesite Unit of the Upper Clarno Formation crops out as a 3 km wide band of andesites that trends north-northeast through the central part of the project area. The unit covers about 23 km^2 and makes up 26 percent of the rocks in the study area. The unit has a total thickness of approximately 830 m and is best exposed south of the prospects in Sec. 35, T. 12 S., R. 19 E., and along the western slopes of lower Dodds Creek valley.

The Quartz-bearing Andesite Unit has a conformable and gradational upper contact with the Pyroxene Andesite Unit of the Upper Clarno and an angularly unconformable lower contact with the Heflin Creek Member lavas of the Lower Clarno. Lava flows of the quartz-bearing andesites do not present the planar, sheet-like aspect character-

istic of lavas of the Lower Clarno. These lavas have undulating contacts and often pinch-out or end abruptly along strike. It is inferred that at least minor topographic relief was maintained while the flows accumulated. The flows making up this unit vary considerably in thickness. Flows in the upper Dodds Creek valley are at least 30 m thick. Thinner flows, making up dip slopes in the SE$\frac{1}{4}$ of Sec. 10, T. 12 S., R. 19 E, vary from 1 to 2 m in thickness. Outcrop characteristics of these lavas are similar to those of the Heflin Creek Member of the Lower Clarno. The lavas are not vesicular and generally lack megascopic flow banding. Platy jointing is well developed on a spacing of from 2 to 7 cm.

Phenocrysts common in handsample are plagioclase, quartz and occasional magnetite and hornblende. Pyroxene, relatively abundant in the other andesites of the Clarno, occurs rarely as recognizable phenocrysts in handsamples of these rocks. The presence of quartz and the absence of pyroxene in handsample is the single most diagnostic criteria for the recognition of this unit in the field.

Colors of fresh and altered samples are similar to those of the andesites of the Lower Clarno. Fresh samples range from medium bluish grey (5B 5/1) to greenish grey (5G 6/1) and weathered exposures are dark greenish grey (5GY 4/1) to olive green (5Y 4/1).

Pilotaxitic and intergranular textures are most commonly displayed by these lavas. Glomeroporphyritic texture, common in most of the Lower Clarno andesites was present in only one of the 11 thinsections of the Quartz-bearing Andesite Unit studied.

In thinsection these rocks are seen to contain a greater variety of phenocrysts than the other lavas of the area. Phenocrysts identified include plagioclase, clinopyroxene, orthopyroxene, hornblende, magnetite and quartz. Although none of the lavas studied contained all of these phases, all of the thinsections contained plagioclase, quartz and at least one ferromagnesian mineral. A volumetric modal analysis of the phenocrystic phases present in these rocks is shown in Table 2.

Plagioclase is usually the predominant phenocryst in the quartz-bearing andesites. It occurs as subhedral to anhedral laths ranging in size from 0.3 mm to 4.0 mm. The plagioclase makes up a maximum of 9 volume percent of the rock and averages 4 percent. The crystals often have borders clouded with magnetite and almost always display the effects of resorption and alteration. Occasionally the altered grains are surrounded by a thin rim of fresh feldspar (Fig. 9). Evidently this outer rim was in equilibrium with the final liquid in the crystalizing melt and was therefore less vulnerable to

Table 2. Volumetric modes of phenocryst phases of selected quartz-bearing andesites, Upper Clarno Formation.

Sample	HS78327	HS7883	HS7875	HS7863	HS7873
Labradorite	8.8%	6.2%	2.0%	2.6%	1.6%
Clinopyroxene	.4%	.4%	tr.	.2%	.2%
Orthopyroxene	-	.2%	-	-	tr.
Hornblende	-	-	2.8%	-	.6%
Quartz	1.4%	2.0%	.6%	.6%	.7%
Magnetite	tr.	.2%	-	tr.	tr.

(tr. = less than .2%)

Sample Locations:

HS78327 Elevation 3,720 ft.; NW¼, SW¼, Sec. 3, T. 11 S., R. 19 E.

HS7883 Elevation 4,120 ft.; NW¼, SW¼, Sec. 16, T. 12 S., R. 19 E.

HS7875 Elevation 3,640 ft.; NE¼, SE¼, Sec. 9, T. 12 S., R. 19 E.

HS7863 Elevation 4,810 ft.; SW¼, SW¼, Sec. 14, T. 12 S., R. 19 E.

HS7873 Elevation 4,080 ft.; NW¼, NW¼, Sec. 15, T. 12 S., R. 19 E.

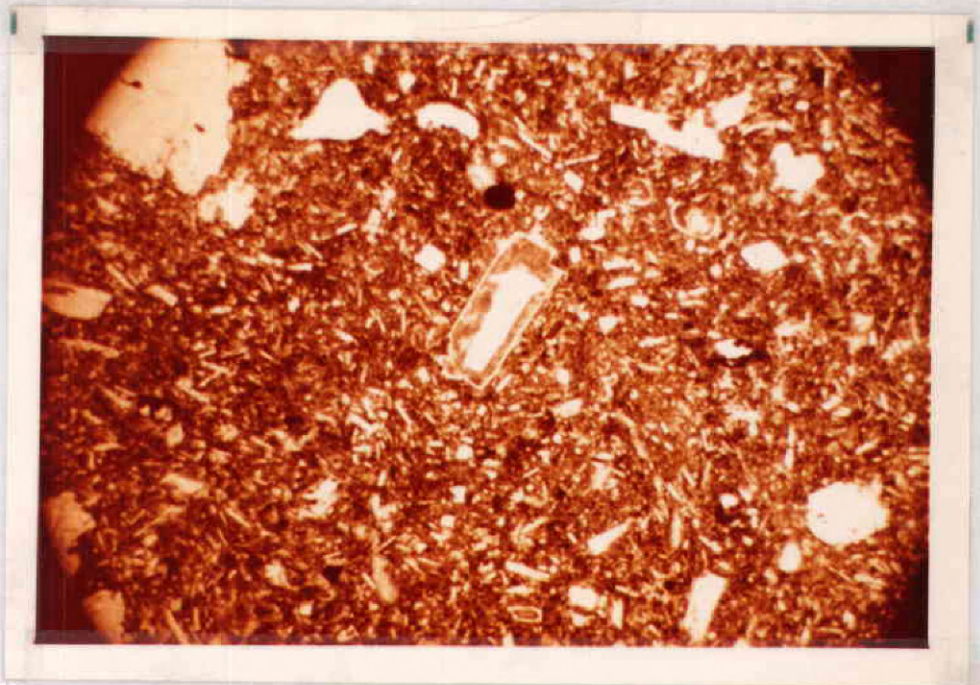

Figure 9. Photomicrograph of quartz-bearing andesite showing altered plagioclase surrounded by unaltered rim. Plane polarized light; field width is approximately 7 mm. (Sample HS78327 from NW$\frac{1}{4}$, SW$\frac{1}{4}$, Sec. 3, T. 11 S., R. 19 E.)

alteration. The plagioclase is labradorite, ranging in composition from An_{52} to An_{61}.

Varieties of zoning displayed by the plagioclase include normal, reverse and oscillatory. Twinning in the plagioclase is by the Albite and Carlsbad laws. It is never well developed and is often obscured by the zoning and resorption. Alteration products of the plagioclase are calcite and clay.

Pyroxenes are never an abundant phenocrystic phase in these andesites. As shown by Table 2, the pyroxenes seldom make up more than 0.5 volume percent of these lavas in thinsection. The pyroxenes present are similar to those of the Heflin Creek Member of the Lower Clarno. The clinopyroxene was again determined to be augite. It occurs as subhedral to anhedral crystals with a maximum size of 1.0 mm. The orthopyroxene is probably hypersthene. Generally it is subordinate in abundance to the clinopyroxene and is totally lacking in some thinsections. Crystals occur as subhedral to anhedral tablets up to 0.7 mm in length. Alteration products of the pyroxenes include magnetite and rarely, chlorite.

Hornblende is present as a phenocryst in a few of these lavas. In most cases it is in various stages of replacement by magnetite, as shown by Figure 10. The hornblende crystals range in size from 0.7 mm to 3.0 mm

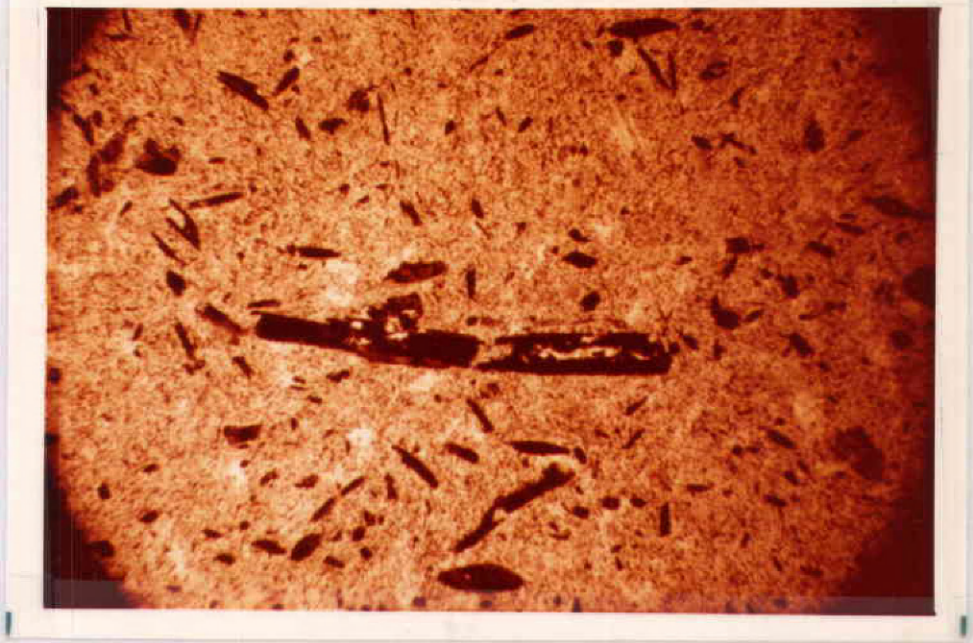

Figure 10. Photomicrograph of quartz-bearing andesite showing hornblende in various stages of replacement by magnetite. Plane polarized light; field width is approximately 7 mm. (Sample HS7875 from NE¼, Sec. 16, T. 12 S., R. 19 E.)

and make up a maximum of 3 volume percent of the rock in thinsection and average 1.5 percent.

Magnetite is large enough in a few of these rocks to be termed a phenocryst. It is present as subhedral to anhedral grains making up a maximum of 0.2 volume of the rock in thinsection.

Quartz is a common phenocryst in these lavas, ranging in abundance from a trace to about 2.0 volume percent. The crystals vary in size from 0.3 mm to 4.0 mm and are always partly resorbed as shown by their rounded and scalloped edges (Fig. 11). Figure 12 shows quartz crystals enclosed in a reaction rim of granular clinopyroxene. Most of the quartz shows this type of reaction rim although the thickness of the rim may vary. Occasionally the pyroxene is separated from the quartz by a thin layer of glass (Fig. 13). As shown by these Figures, almost all of the quartz is cut by irregular fractures. Wright and Larsen (1909) noted that fracturing is characteristic of quartz that has undergone thermo-mechanical stress from the eruptive process. In the quartz of some of the lavas these fractures are stained with hematite, giving the quartz a reddish color in handsample.

Groundmass constituents of these lavas include plagioclase, the two pyroxenes, and magnetite. These

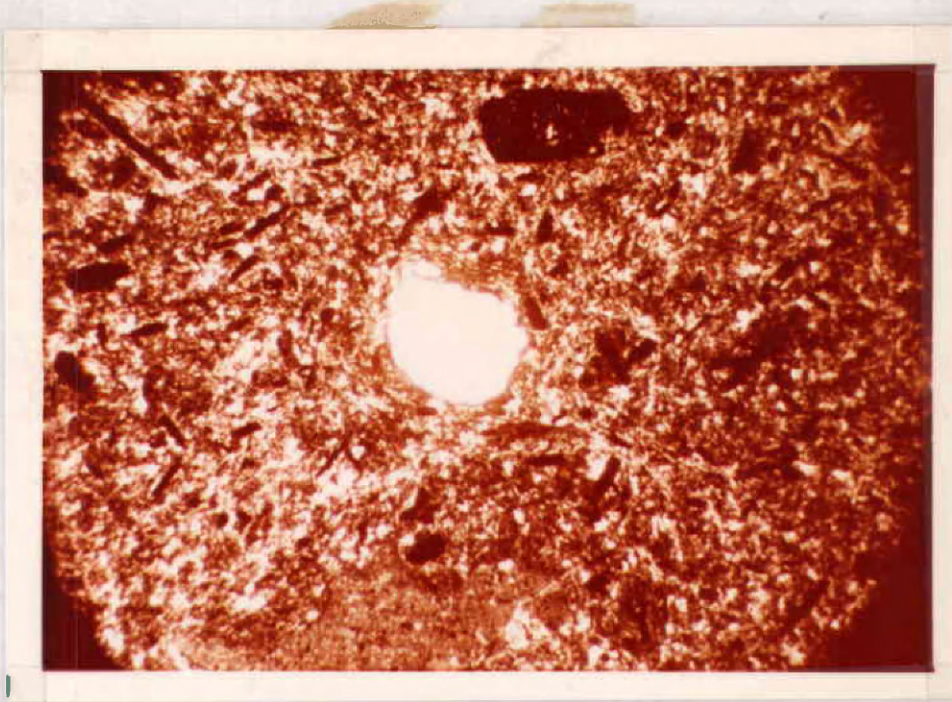

Figure 11. Photomicrograph of quartz-bearing andesite showing resorbed quartz crystal with scalloped edges. Cross polarized light; field width is approximately 7 mm. (Sample HS7875 from NE¼, Sec. 16, T. 12 S., R. 19 E.)

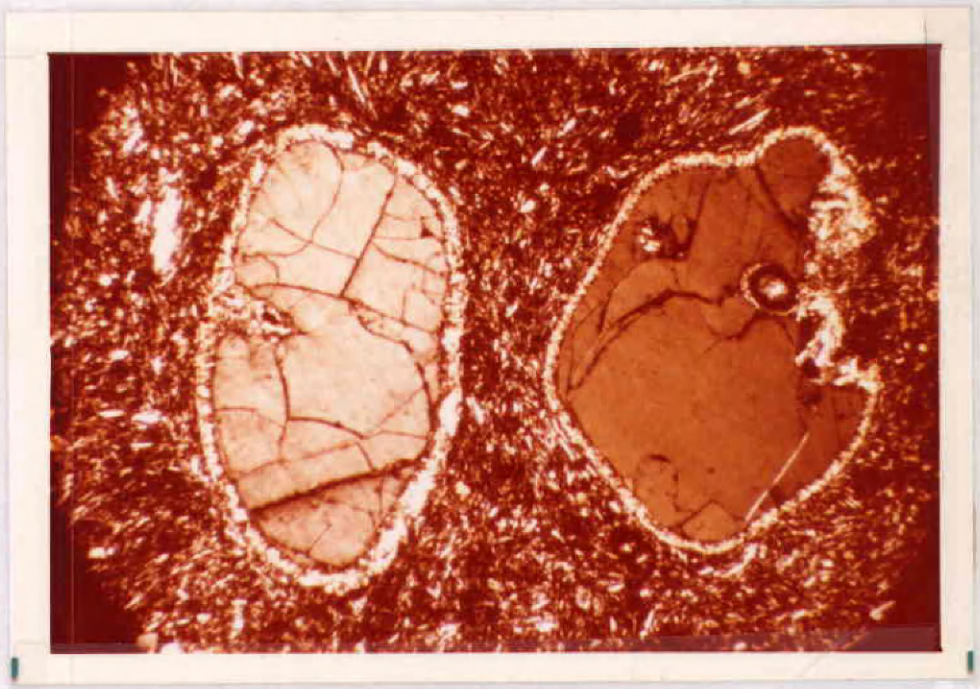

Figure 12. Photomicrograph of quartz-bearing andesite showing quartz crystals rimmed by granular clinopyroxene. Cross polarized light; field width is approximately 7 mm. (Sample HS7881 from SW¼, Sec. 16, T. 12 W., R. 19 E.)

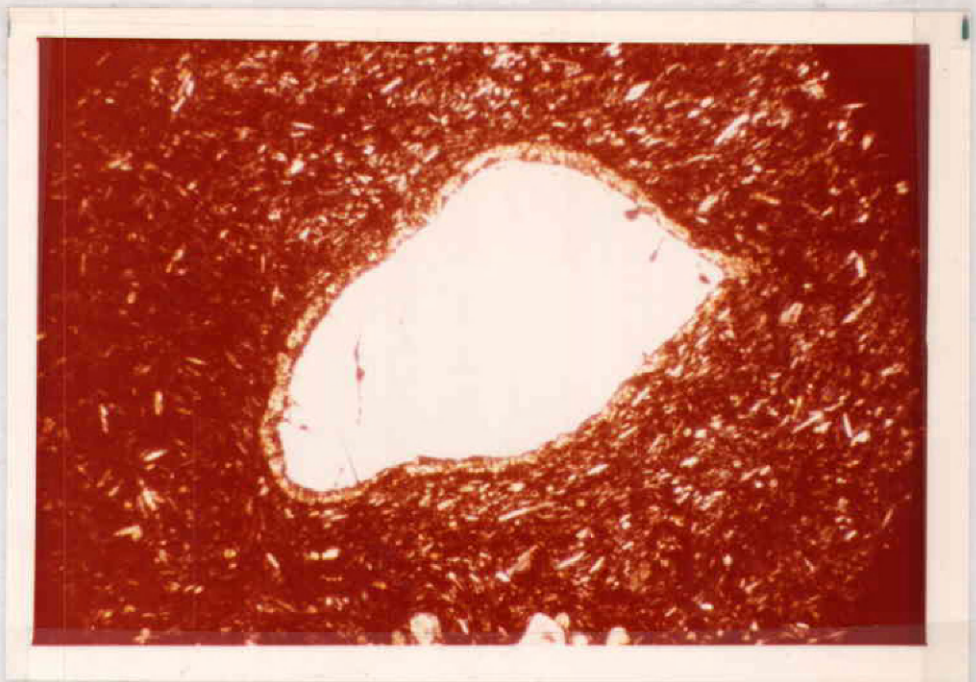

Figure 13. Photomicrograph of quartz-bearing andesite showing a resorbed quartz crystal with a reaction rim of glass and clinopyroxene. Cross polarized light; field width is approximately 7 mm. (Sample HS7881 from SW$\frac{1}{4}$, Sec. 16, T. 12 S., R. 19 E.)

minerals generally show alteration similar to that displayed by the phenocrysts. The plagioclase forms euhedral to subhedral laths up to 0.3 mm in length. The crystals range in composition from calcic andesine to sodic labradorite (An_{42}-An_{53}) and make up from 50 to 75 volume percent of the rock. The groundmass pyroxenes were too small to be positively identified but are probably augite and hypersthene. Together the two pyroxenes make up from 7 to 28 volume percent of the andesite. Groundmass magnetite varies in abundance from 2 to 6 volume percent as subhedral to anhedral crystals.

The occurrence of resorbed quartz in calc-alkaline volcanic rocks is well documented (Nicholls et al., 1971). The origin of the quartz, however, is imperfectly understood. Rittman (1962), in a discussion of dacitic magmas, states that corroded quartz grains are not magmatic precipitates but refractory components that have survived anatexis. Steiner (1963) uses the antipathetic relationship between hypersthene and quartz (Bowen, 1928) to support his hypothesis of a xenocrystic origin for the quartz in a hypersthene-bearing ignimbrite of New Zealand. Moorehouse (1959) has noted resorbed quartz surrounded by reaction rims of pyroxene in the San Juan Lavas of Colorado. He strongly favors a xenocrystic origin for the quartz stating (p. 207-208):

> "In these, angular, sometimes corroded chips and fragments of quartz, feldspar and ferromagnesian minerals occur in a glassy or microcrystalline matrix of acid composition. It is as if the lava of matrix had picked up innumerable fragments of wall rock and incorporated them with very little effect on itself."

Although some occurrences of resorbed quartz may be explained by hypotheses of xenocrystic origin, the nearly uniform size and distribution of the quartz in the lavas of the study area would seem to demand a less random, more uniform origin. The work of Tuttle and Bowen (1958) on the system $NaAlSi_3O_8$-$KAlSi_3O_8$-SiO_2-H_2O suggests such a mechanism. Tuttle and Bowen found that an increase in PH_2O in the system would produce an increase in the stability field of quartz at the expense of the feldspars. The effect is to change the position of the eutectic in the quartz-feldspar binary system. Hence quartz, crystallizing from a magma of appropriate composition would, with a reduction of water vapor pressure, no longer be in equilibrium with the melt and would undergo resorption. This mechanism has been proposed by Ewart (1965) to account for resorbed quartz phenocrysts in a New Zealand ignimbrite. Green and Ringwood (1968a), however, point out that such a mechanism would raise the liquidus temperature of the system causing an increase in crystallization. Resorption, they suggest, would be a second-order feature. Their

work suggests that resorbed quartz in calc-alkaline magmas is formed at high pressures under dry conditions. On cooling, the quartz is replaced by feldspar as the liquidus phase and resorption of the quartz occurs. As noted by Steiner (1963), quartz is an extremely refractory mineral. If a quartz-bearing magma were to ascend rapidly to the surface quartz phenocrysts would not completely be resorbed. This hypothesis of rapid ascent is supported by the lack of abundant phenocrysts in the quartz-bearing andesites.

Nicholls et al., (1971) suggest that many so called quartz xenocrysts in calc-alkaline magmas may be of cognate origin and stable at elevated pressures. Assuming equilibration temperatures of 1000° and 1100°C and a dry magma of basaltic andesite composition they have calculated that at pressures of 16 Kb to 27Kb the quartz would be in equilibrium. The occurrence of garnet (?) in the lavas overlying the Quartz-bearing Andesite Unit also suggests a deep origin for the magmas producing these rocks (Green and Ringwood, 1968a).

Pyroxene Andesite Unit

The pyroxene andesites of the Upper Clarno Formation are the most abundant rocks of the project area. These lavas cover about 32 km^2 and make up 36 percent of the rocks in the area studied. Exposures of flows

characteristic of this unit can be seen north of the prospects in Sec. 35, T. 11 S., R. 19 E. This member conformably overlies the Quartz-bearing Andesite Unit of the Upper Clarno. The upper contact of this unit is not exposed within the bounds of the project area. The thickness of the unit within the project area is about 700 m.

The flows making up this unit cannot be traced over broad areas and are often quite variable in thickness. The thickest flows observed are at least 30 m thick and are located in the N½, Sec. 31, T. 11 S., R. 19 E. Thinner flows, varying from 1 to 5 m in thickness are found on the east-west trending ridge in the N½, Sec. 8, and 9, T. 12 S., R. 19 E. These thin flows often have brecciated and deeply weathered upper and lower contacts as shown in Figure 14. Lavas of pyroxene andesite of the Upper Clarno Formation are generally nonvesicular and lack megascopic flow banding. Platy jointing, producing curved plates 1 to 5 cm thick, is well developed in all of the thicker flows of this unit.

Fresh samples of the lava making up this unit are generally a dark greenish grey (5GY 4/1). Weathered surfaces are olive grey (5Y 4/1) to dark greenish grey (5GY 4/1). The joint surfaces of the rock are often stained a light brown (5YR 5/6) by hematite. This

Figure 14. Photograph of thin lava flow of Pyroxene Andesite Unit showing weathered upper and lower contacts. Hammer for scale. (NW$\frac{1}{4}$, Sec. 8, T. 12 S., R. 19 E.)

feature is poorly developed in the other andesites and, when present, permits recognition of the unit from a distance.

These andesites are very similar in thinsection to the andesites of the Heflin Creek Member of the Lower Clarno Formation and only exceptional features will be discussed here. The dominant textures developed in these rocks are pilotaxitic and glomeroporphyritic. Intergranular texture is displayed by the lavas containing abundant groundmass pyroxene.

All of these andesites are porphyritic with plagioclase, clinopyroxene and orthopyroxene. Magnetite occurs as a phenocryst in a few of the flows. A volumetric modal analysis of the phenocrystic phases present in thinsection is shown in Table 3.

The plagioclase phenocrysts in these lavas vary in length from 0.6 mm to 1.8 mm. These crystals make up a maximum of 18 volume percent of the rock and average 14 volume percent. The crystals are labradorite, ranging between An_{54} and An_{63}. Many of the plagioclase phenocrysts in these lavas show the effects of corrosion and resorption. The resorption cavaties are commonly filled by magnetite or other plagioclase (Fig. 15). Vance (1965) attributes this corrosion and patchy zoning in plagioclase to reactions taking place in water-deficient magmas during their ascent to the surface. He

Table 3. Volumetric modes of phenocryst phases of selected pyroxene andesites, Upper Clarno Formation.

Sample	HS7845	HS7884	HS7885	HS7888	HS7890
Labradorite	18.2%	16.1%	16.3%	13.9%	11.3%
Clinopyroxene	1.7%	6.1%	3.6%	1.7%	.6%
Orthopyroxene	2.0%	.8%	5.0%	2.0%	3.4%
Magnetite	-	tr.	-	-	-

(tr. = less than .2%)

Sample Locations:

HS7845 Elevation 3,500 ft.; NE¼, SE¼, Sec. 34, T. 11 S., R. 19 E.

HS7884 Elevation 4,620 ft.; SW¼, NE¼, Sec. 18, T. 12 S., R. 18 E.

HS7885 Elevation 4,300 ft.; SE¼, SW¼, Sec. 17, T. 12 S., R. 19 E.

HS7888 Elevation 4,300 ft.; SE¼, NE¼, Sec. 8, T. 12 S., R. 19 E.

HS7890 Elevation 4,710 ft.; SE¼, NE¼, Sec. 7, T. 12 S., R. 19 E.

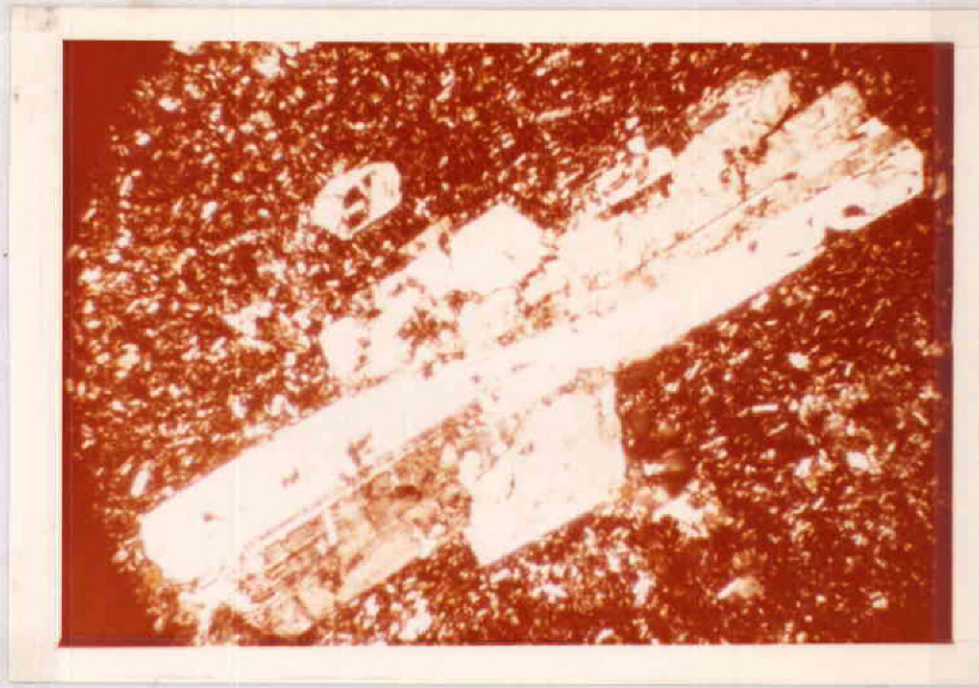

Figure 15. Photomicrograph showing patchy zoning in plagioclase of the Pyroxene Andesite Unit, Upper Clarno Formation. Cross polarized light; field width is approximately 7 mm. (Sample HS7890 from NE$\frac{1}{4}$, Sec. 7, T. 12 S., R. 19 E.)

states (p. 646):

> "With fall in pressure at nearly constant temperature, both liquidus and solidus are depressed. To reestablish equilibrium, the melt must become richer in anorthite, a condition which will tend to be reached by resorption of plagioclase crystals already present."

Less-calcic plagioclase, crystalizing at lower temperature is deposited in the resorption cavities and forms rims about the crystals giving a patchy texture. Vance also noted an abundance of inclusions of other minerals in plagioclase displaying patchy zoning. These inclusions represent products of the melt that became trapped within the corrosion cavities following resorption.

The pyroxene phenocrysts in these lavas were again determined to be augite and hypersthene. The augite is subhedral and varies in length from 0.6 mm to 2.5 mm. It makes up a maximum of about 6 volume percent of the rock and averages 3 volume percent. The orthopyroxene ranges in length from 0.4 mm to 1.0 mm as anhedral to subhedral grains. It makes up a maximum of 3.4 volume percent and averages 2.7 percent.

Phenocrystic magnetite occurs in trace amounts in two of the thinsections studied. It is anhedral and ranges in size from 1.5 to 2.0 mm.

The predominant groundmass constituents of these andesites are plagioclase, the two pyroxenes and mag-

netite. The plagioclase makes up from 55 to 70 volume percent of the rock and ranges in composition from andesine to sodic labradorite (An_{42}-An_{52}). The pyroxenes make up a maximum of 22 volume percent and average 16 percent. Magnetite makes up the remainder, averaging 3 volume percent.

Two of the thinsections of pyroxene andesite examined contain groundmass crystals which have been tentatively identified as garnet. The samples containing these crystals were taken from outcrops located in a roadcut at an elevation of 4,280 feet in the NW¼, SE¼, SW¼, Sec. 17, T. 12 S., R. 19 E. and on the northwestern slopes below Cougar Butte at an alevation of 4,720 feet in the NE¼, SE¼, SE¼, Sec. 15, T. 12 S., R. 19 E. Although the later sample was taken from the area mapped as part of the Quartz-bearing Andesite Unit of the Upper Clarno Formation, the rock containing the garnet is a pyroxene andesite. This situation is a result of the gradational contact between these two units and the manner in which the boundary between them is defined.

The crystals identified as garnet range in size from 0.01 mm to 0.03 mm and occur as euhedral to subhedral, equant, six-sided crystals (Fig. 16). The crystals are isotropic and are dark pink in plain polarized light.

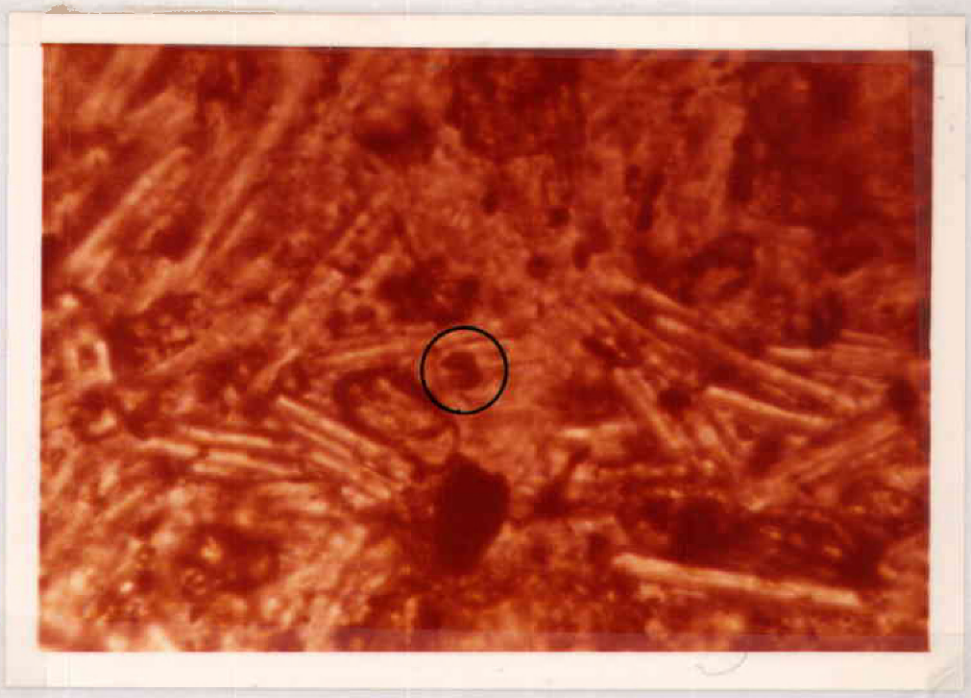

Figure 16. Photomicrograph of pyroxene andesite showing garnet (?) (circled). Plane polarized light; field width is approximately 0.15 mm. (Sample HS7864 from NW$\frac{1}{4}$, SE$\frac{1}{4}$, SW$\frac{1}{4}$, Sec. 17, T. 12 S., R. 19 E.)

Although the identification is only tentative, a few points in connection with the occurrence of garnet in andesites are worthy of mention. Green and Ringwood (1968b) point out that garnet phenocrysts are typically associated with resorbed quartz phenocrysts in calc-alkaline rocks. Although quartz and garnet have not been found occurring together in these rocks, the nature of the boundary between the Upper Clarno andesitic units suggest that the two units may be comagmatic. This is supported by the similar chemistry displayed by the lavas of the two units. Green and Ringwood (1968a) also note that garnet is a liquidus or near-liquidus phase in calc-alkaline andesites at a pressure of from 27Kb to 37Kb. As mentioned in a previous section of this study, resorbed quartz phenocrysts also suggest a deep origin for the Upper Clarno lavas. It is interesting to note that both of these lines of evidence call for crystallization from water-deficient magmas. This is in accord with the conditions proposed by Vance (1965) to account for the patchy zoning of the type displayed by the plagioclase in these andesites.

Rhyolite Flows

The rhyolite flows of the Upper Clarno Formation occur on the southern slopes of Stephenson Mountain in the northcentral part of the project area and in

the vicinity of Rooster Rock to the southwest. The flows cover about 9 km^2 and make up 10 percent of the rocks in the study area. The maximum thickness of the lavas is on the order of 200 m. The rhyolites form flat-topped mesas bounded by steep-sided cliffs up to 70 m high. It is uncertain how many individual flows are included in the exposures but the "terraced" nature of the outcrops on the southeastern slopes of Stephenson Mountain suggest that at least four are involved. In plan view, the rhyolite flows on these slopes are elongate in a northeast direction and, as shown by Figure 17, the flows have a lower contact which is concave upward. These facts suggest that the rhyolites filled northeast trending canyons which were eroded in the Upper Clarno andesites. Fragments of olive black (10YR 6/2) vitrophyre can be found near the base of many of the flows and the upper parts of the flows often contain abundant vugs. Flow banding, defined by different colored lenses of rhyolite, is a common feature in all of these flows. Out crops of the rhyolite are often cut by vertical joints spaced at 3 to 7 m and occasionally display a platy jointing on a spacing of from 2 to 7 cm. Hand-samples of fresh rhyolite vary from yellowish grey (5Y 8/1) to light brownish grey (5YR 6/1) and weathered samples are generally pale yellowish brown (10YR 6/2).

Figure 17. Photograph of the rhyolite flows making up the south western slopes of Stephenson Mountain. The cliffs are about 70 m high. (Sections 32 and 33, T. 11 S., R. 19 E.)

Less than 1 km southeast of the rhyolite flows are several rhyolite dikes which have intruded the pyroxene andesites of the Upper Clarno. The work of Owen (1977) points out the chemical similarities between the dikes and the flows. The two are probably comagmatic and the dikes may have served as feeders for the flows.

In thinsection the rhyolite flows are seen to contain phenocrysts of quartz, plagioclase, sanidine and biotite in a groundmass displaying well developed flow banding (Fig. 18). The phenocrysts are anhedral to subhedral and generally less than 1.0 mm in diameter. They make up less than 1 volume percent of the rock and often occur in clusters of two or more crystals. The plagioclase is oligoclase (An_{24}-An_{28}).

The groundmass of the rock consists almost entirely of devitrified glass. Although the products of devitrification have not been positively identified they are probably quartz and alkali feldspar. Trace amounts of magnetite are found in the groundmass. Some of the magnetite has been oxidized to hematite, coloring parts of the rock a pale orange.

Intrusive Rocks: Introduction

Four megascopically different types of intrusive rock are present in the project area. On the basis of chemical composition two of the types are andesite,

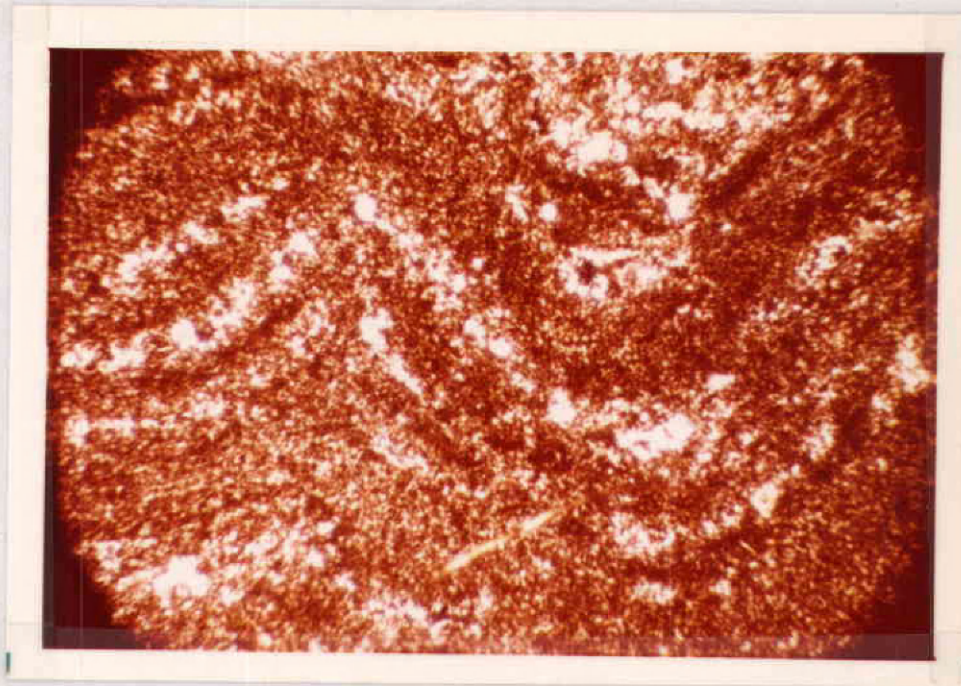

Figure 18. Photomicrograph of Upper Clarno rhyolite flow showing well developed flow banding. Plane polarized light; field width is approximately 7 mm. (Sample HS7811 from NW¼, SW¼, Sec. 33, T. 11 S., R. 19 E.)

one is dacite and one is rhyolite. The andesites are the most abundant of the intrusive types and dacites are the least abundant. Representative analyses of these rocks are presented in Appendix A.

Andesite Intrusions

The andesite intrusions are divided into two groups, the porphyritic andesites and the glassy andesites. Although the two varieties are chemically similar, they are easily distinguished from one another in handsample and thinsection. The porphyritic andesites are more abundant than the glassy variety and will be discussed first.

The porphyritic andesites generally occur as nearly circular plugs up to .6 km in diameter. The intrusions are more resistant to erosion than the surrounding lavas and, as shown by Figure 19, often stand out in relief. The plugs generally display a blocky jointing or fracture rather than the platy jointing seen in the lavas. Fresh surfaces of the rock vary from pale yellowish brown (10YR 6/2) to dusky yellowish brown (10YR 2/2). Weathered exposures are more variable, but include light olive grey (5Y 5/2), moderate olive brown (5Y 4/4) and greyish olive (10Y 4/2).

In thinsection the porphyritic andesites are very similar to the lavas of the Pyroxene Andesite Unit of

Figure 19. Photograph of porphyritic andesite intrusions. The intrusions have weathered into relief about 40 m. (NE$\frac{1}{4}$, Sec. 36, T. 11 S., R. 19 E.)

the Upper Clarno Formation. Intergranular texture is very common in these rocks. Pilotaxitic and glomeroporphyritic textures are also present but not as well developed as in the lavas. Phenocrysts present in these rocks include plagioclase, clinopyroxene, orthopyroxene and magnetite.

The plagioclase phenocrysts occur as euhedral to subhedral tabular crystals up to 4.0 mm in length. They make up a maximum of 18 volume percent and average 15 percent. Albite and Carlsbad twins are common and varieties of zoning developed include normal, reverse, oscillatory and patchy. The phenocrysts are labradorite, ranging from An_{52} to An_{56}.

The pyroxene phenocrysts in the rock are, on the basis of optic sign and 2V, thought to be augite and hypersthene. Both pyroxenes occur as euhedral to subhedral tablets up to 1.5 mm in length. The augite makes up a maximum of 2 volume percent and averages 1.7 percent. Hypersthene is more abundant, making up a maximum of 3 volume percent and averaging 2.5 percent.

Many of the orthopyroxene phenocrysts are rimmed by minute grains of clinopyroxene (Fig. 20). Huggins (1978) reported similar occurrences in the andesites of the Painted Hills Quadrangle to the northeast and attributes the rims to late magmatic or deuteric reactions. This conclusion is supported by the corroded and resorbed

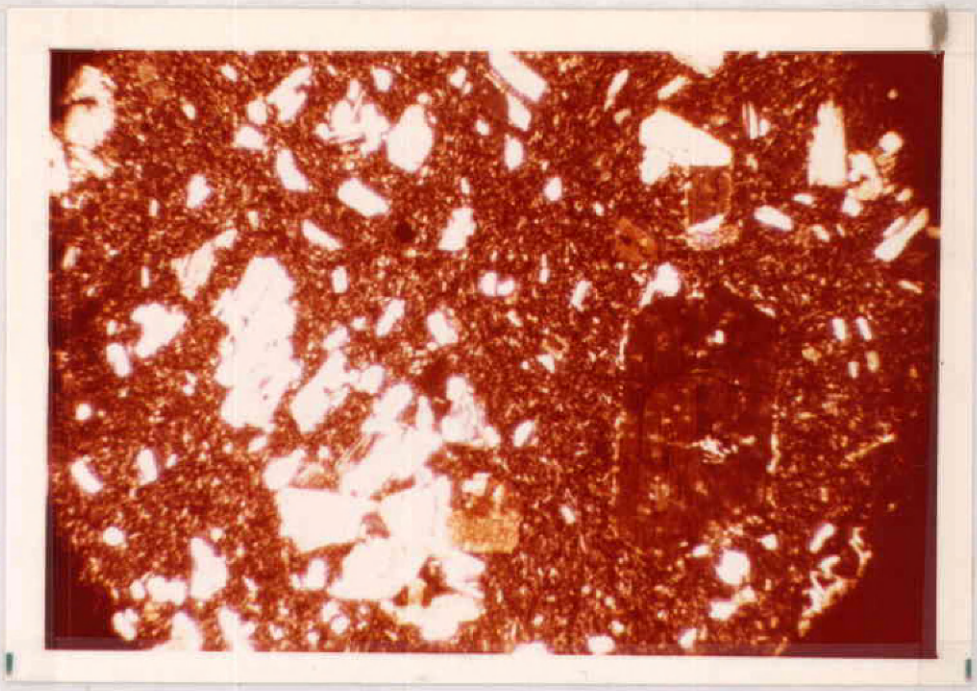

Figure 20. Photomicrograph of porphyritic andesite intrusive rock showing orthopyroxene phenocryst rimmed by granular crystals of clinopyroxene. Cross polarized light; field width is approximately 7 mm. (Sample HS7841 from intrusion in NE¼, Sec. 36, T. 11 S., R. 19 E.)

borders of the orthopyroxene crystals seen in these rocks. Kuno (1950) arrived at a similar conclusion for rimmed pyroxenes from the Halokone Volcano in Japan.

Magnetite phenocrysts are scattered throughout the rock as subhedral to anhedral grains up to 0.1 mm in size. The grains make up a maximum of 0.5 volume percent of the rock and average 0.2 percent.

Groundmass constituents of the porphyritic andesites include plagioclase, clinopyroxene, orthopyroxene and magnetite. The plagioclase is andesine (An_{38}-An_{46}) and makes up from 45 to 70 volume percent of the rock. The two pyroxenes comprise an average of 18 volume percent of the rock and magnetite averages 4.0 volume percent.

The glassy andesites occur as both plugs and dikes. The plugs are very small; the largest has a diameter of .3 km. Most of the plugs are found in the northwestern part of the project area within the crush zone of a major east-west trending fault and, as shown in Figure 21, are extremely fractured. It is possible that these plugs represent fragments of larger intrusions that were emplaced along the fault early in its formation and have been broken up by subsequent movement along it. This hypothesis is supported by the occurrence of megascopically similar xenoliths (Fig. 22) in all of the plugs. Many of these xenoliths, especially the smaller ones, have been fused to a black glass. The

Figure 21. Photograph of glassy andesite intrusion. Hammer for scale. (SE$\frac{1}{4}$, Sec. 32, T. 11 S., R. 19 E.)

Figure 22. Photograph of pyroxene andesite showing xenoliths. Pencil for scale. (X$\frac{1}{2}$, Sec. 34, T. 11 S., R. 19 E.)

larger, unfused xenoliths are angular, and on the basis of their minerology, are thought to be fragments of pyroxene andesite lava of the Upper Clarno Formation.

Several glassy andesite dikes are found in the project area. A group of five of these dikes is concentrated in a 1 km^2 area 1 km southwest of the largest glassy andesite plug Sec. 6, T. 11 S., R. 19 E. Dikes in the group trend north to northwest. They dip from near vertical to 75° to the east and vary in width from 3 to 15 m. Strike-slip faults cut the dikes and the longest continuous segment exposed is .8 km long. The thicker sections of the dikes display horizontal columnar jointing. The columns are three to five sided and up to 30 cm wide and 3 m long. Usually the dikes lack the columnar jointing and are instead cut by irregular fractures which parallel the contacts. Several of these dikes contain xenoliths similar to those observed in the glassy andesite plugs to the northeast.

Two other dikes of glassy andesite are found in the area. The larger of the two is found in the southeastern corner of the project area east of Dodds Creek. This dike is exposed for a distance of about 1.6 km and has a width of up to 90 m. It trends to the north-northeast and dips near vertically. As shown in Figure 23, the dike displays very well developed horizontal columnar jointing. The columns are four and five sided,

Figure 23. Photograph of a glassy andesite dike showing well developed horizontal columnar jointing. The columns in this photo average 3.5 m wide. (NW¼, Sec. 18, T. 12 S., R. 20 E.)

and up to .6 m wide and 6 m in length.

The remaining dike of glassy andesite is found north of the Stephenson Ranch Headquarters in the northeast corner of the area. The dike trends east-northeast and dips from near vertical to 70° to the north. It has a length of almost .9 km and varies in width from 1 to 6 m. Poorly developed horizontal columns extend across the width of the dike. In several places the dike has been offset a few meters by minor faults.

Outcrops of glassy andesite are very distinctive in the field. The rock is extremely hard and resistant to erosion and often protrudes well above the surrounding rocks. Fresh surfaces of the rock are a dark grey (N3) to a greyish black (N2) and weathered exposures are bleached a medium bluish grey (5B 5/1).

In thinsection the glassy andesites are very similar to the porphyritic andesites. The main difference between the two types of intrusive andesite is the relative proportion of phenocryst versus groundmass phases; these andesites are markedly less porphyritic. Plagioclase makes up an average of 9 volume percent as euhedral to subhedral crystals. Clinopyroxene and orthopyroxene make up an average of 0.6 and 0.7 volume percent, respectively, as euhedral to subhedral tablets. Magnetite is the only phenocryst more abundant in these rocks than in the porphyritic andesite intrusions. It

makes up an average of one volume percent and often has a well developed euhedral form. Brown glass accounts for 30 to 40 volume percent of the rock and the remaining percentage is made up of the groundmass phases of plagioclase, magnetite, and the two pyroxenes.

In comparing the two types of intrusive andesite several generalizations are apparent. The porphyritic andesites: 1) always occur as plugs, and 2) are markedly similar, lithologically, to the pyroxene andesite lavas of the Upper Clarno Formation. The glassy andesites: 1) occur as dikes and small plugs, 2) are only slightly porphyritic, 3) often contain numerous xenocrysts, and 4) are often associated with fractures and faults. From these generalizations it is inferred that the porphyritic andesites may represent magmas that cooled at deep levels, possibly in a plutonic or subvolcanic environment. The glassy andesites, on the other hand, may represent magmas which ascended rapidly from depth along faults and fissures and cooled near the surface. Several of the glassy andesite intrusions have been cut by movement along the faults they intruded.

Dacite Intrusions

One small dacite plug is exposed in the project area. The plug intrudes pyroxene andesite of the Upper

Clarno Formation in NE¼, Sec. 17, T. 12 S., R. 19 E. The intrusive has a maximum diameter of about 250 m and is slightly elongate in a northeast direction. Poorly developed columnar joints are displayed by the intrusive near its southwest margin. In general, however, the intrusive lacks any consistent jointing and is, instead, cut by randomly oriented fractures. Fresh samples of the rock are a dark grey (N2) to black (N1). Weathered exposures are bleached to a medium bluish grey (5B 5/1) and joint surfaces are occasionally oxidized to a moderate reddish orange (10R 6/6).

The rock making up the intrusive is very glassy and breaks with a conchoidal fracture. In thinsection it is seen to contain phenocrysts of plagioclase, magnetite, clinopyroxene, and orthopyroxene which together make up less than one volume percent of the rock. The plagioclase phenocrysts are euhedral to subhedral, up to 1.0 mm in length, and are at least as calcic as An_{42} (andesine). This value must be considered a minimum, however, because it was determined by the stastical method of Michael-Levy on a very limited number of crystals. The pyroxenes in the rock are subhedral to anhedral, up to 0.7 mm in length, and generally resorbed. Phenocrystic magnetite is present as euhedral to subhedral crystals up to 0.2 mm in diameter.

The groundmass of the rock is dominated by plagioclase microlites and glass. The microlites account for 45 to 55 volume percent of the rock and are andesine (An_{36}-An_{38}). The parallel allignment of these crystals gives the rock a pilotaxitic texture. Clear glass makes up about 35 volume percent and minute crystals of magnetite and pyroxene account for the remainder.

Rhyolite Intrusions

Two small rhyolite plugs and several rhyolite dikes intrude the andesites of the Upper Clarno. The plugs are located near the margin of an andesitic intrusion in NE$\frac{1}{4}$ of Sec. 36, T. 11 S., R. 19 E. Both plugs are relatively small; the larger of the two has a maximum diameter of about 60 m. The rhyolite dikes are part of a northeast trending swarm reported by Owen (1977). They are located on the southern slopes of Stephenson Mountain in the northcentral part of the project area. As shown by Figure 24 the light colored dikes stand out in sharp contrast against the darker colored andesites. Within the project area the dikes are up to .2 km long and 125 m wide. As shown by the work of Owen (1977), these dikes are similar, chemically, to the rhyolite flows on Stephenson Mountain. This suggests that the dikes may have served as feeders for the flows.

Fresh surfaces of the intrusive rhyolite are white

Figure 24. Photograph of rhyolite dike intruded into the pyroxene andesites of the Upper Clarno. The dike is approximately 100 m wide. (NE$\frac{1}{4}$, Sec. 34, T. 11 S., R. 19 E.)

(N9) to very light grey (N8). Weathered exposures of the rock are often oxidized to various shades of red.

In thinsection the intrusive rocks appear to be composed almost entirely of blebs and veins of quartz, glass, and plagioclase microlites. The quartz occurs as anhedral grains which are scattered throughout the rock. The grains are elongated and display a preferred orientation which gives the rock a banded appearance in handsample. The plagioclase microlites are probably a product of devitrification of the volcanic glass and are too small to be compositionally identified by the optical methods used.

Biotite, plagioclase and sanidine were the only phenocrysts found. The phenocrysts occur as subhedral to anhedral crystals up to 0.7 mm in length and together make up less than one volume percent of the rock. The sanidine is distinguished from the quartz only by its negative optic sign and a slightly biaxial character. The plagioclase phenocrysts are not present in sufficient quantities to allow an accurate optical determination of their composition. Owen (1977), however, examined thinsections from these dikes which contained a greater proportion of phenocrysts and arrived at a composition of albite (An_6-An_{10}) for the plagioclase.

Quaternary Deposits

Four types of Quaternary deposits are found in the project area. The most extensive are landslides which cover a total of about 6.5 km^2. The larger slides are composed mainly of debris from the rhyolite flows. These slides and their remnants cover parts of : Sections 3, 4, 5, 17, and 18, T. 12 S., R. 19 E., and Sections 32 and 33, T. 11 S., R. 19 E. These slides probably result from collapse of the over-steep slopes produced by vertical jointing in the rhyolite flows. A smaller slide, composed mainly of andesite, is found in parts of Sections 2 and 3, T. 12 S., R. 19 E. The cause of this slide is unknown. On aerial photographs the landslides are very distinctive; they appear as low, hummocky surfaced, undulating hills.

The second most extensive of the Quaternary deposits is stream alluvium. It is found in most of the valleys and larger gullies, especially those with perennial streams. The alluvium consists of poorly sorted, unconsolidated material washed down from the surrounding slopes. Judging from the topography of the area, the deposits often have a thickness of several meters. Much of the alluvium in the area is undergoing active erosion.

The third most extensive of the Quaternary deposits,

as depicted on Plate 1, are talus deposits. The deposits are well developed below the ignimbrite and steep-sided flows and intrusive bodies. Talus is depicted on Plate 1 where it differs lithologically from the underlying bedrock; or is similar but exceeds an area greater than .25 km^2.

The last category of Quaternary deposits in the area results from the process of slumping. The slumps occur adjacent to Bear Creek in the NW$\frac{1}{4}$ of Sec. 2, T. 12 S., R. 19 E., and consist of lava blocks which have moved downslope short distances as coherent units. The blocks have, in most cases, undergone slight rotation but are distinct from the chaotic mass of rock and soil which characterize the landslides of the area. The slumps probably result from undermining of the lavas by Bear Creek.

GEOCHEMISTRY

The rocks of the project area range in chemical composition from andesitic to rhyolitic. The chemical analyses and sample locations of rocks analyzed are shown in Appendix A. These analyses augment the geochemical data of Barnes (1978) and Huggins (1978) which are also presented in Appendix A. The combined data provide a broader data base and the interpretations presented are more meaningful than was possible with the results of this study alone. Together the three studies provide a series of rocks which range in composition from basaltic andesite with 55 weight percent silica to rhyolite with 74 weight percent silica.

When plotted on Harker diagrams (Appendix B) the major element oxides display trends typical of calc-alkaline rocks. With increasing silica content the concentrations of Na_2O and K_2O increase and the concentrations of MgO, FeO, CaO, Al_2O_3 and TiO_2 decrease.

The Clarno rocks are calcic when plotted on a Peacock diagram, giving an alkali-lime index of 62 (Fig. 25). Barnes (1978) suggests that this calcic character is the result of calcium enrichment due to Ca-bearing alteration products. Although alteration has undoubtedly affected the chemistry of these rocks, the slight degree of scatter seen on the Ca-SiO_2 var-

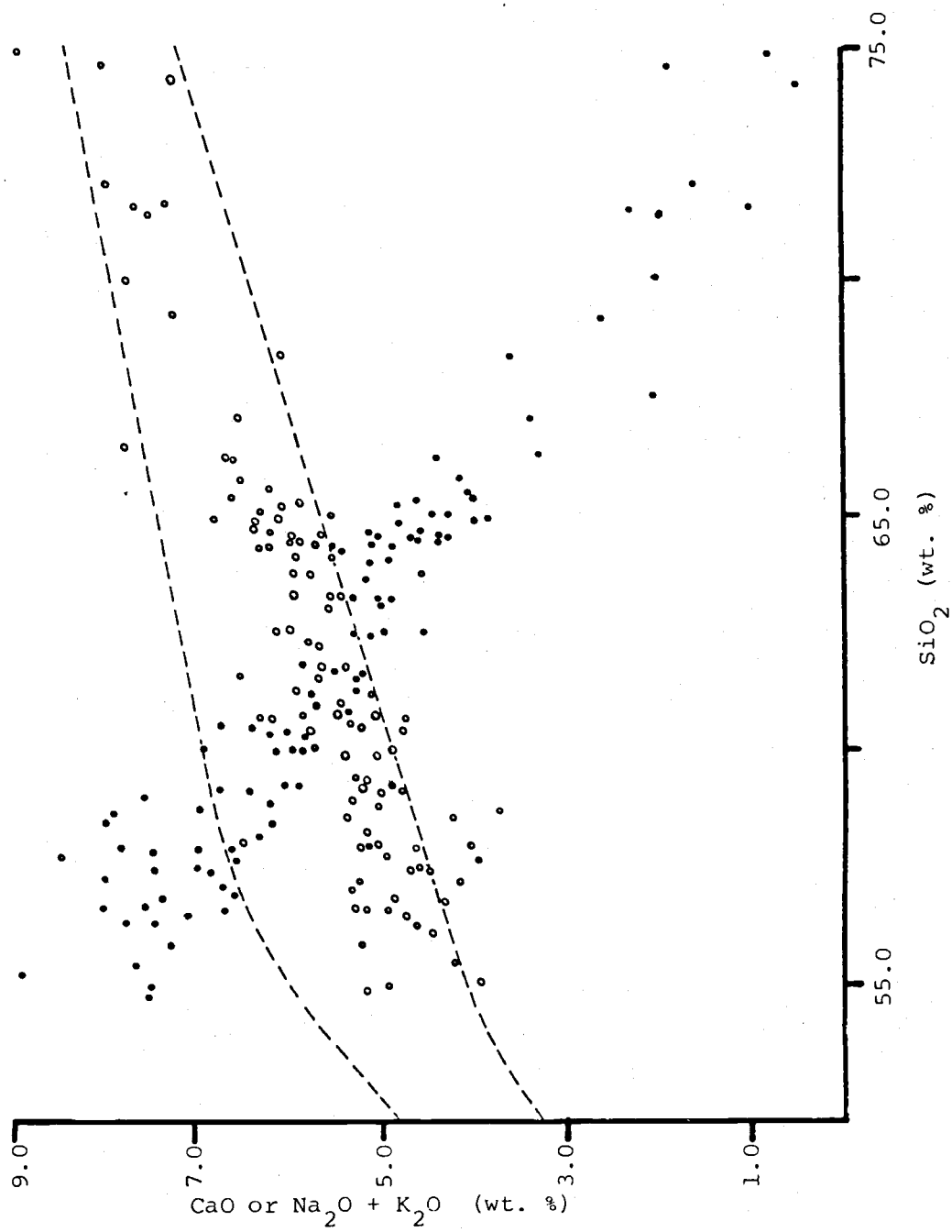

Figure 25 - "Peacock Diagram" of Clarno rocks.

Solid circles represent weight percent CaO vs. SiO_2; hollow circles represent weight percent Na_2O+K_2O vs. SiO_2. The two curved, dashed lines represent Kuno's (1966) high-alumina basalt field.

iation diagram argues against any major shift in the alkali-lime index. As noted by Taylor (1977, in Huggins 1978) this low degree of scatter seen on CaO-SiO_2 variation diagrams is characteristic of Clarno rocks. When evaluated by other parameters the Clarno rocks show distinct calc-alkaline affinities. As shown by Figure 26 the Clarno rocks follow a calc-alkaline trend, showing no marked iron enrichment. Also as noted by Rogers and Novitsky-Evans (1977) the K_2O-SiO_2 slope of Clarno rocks places them in the calc-alkaline assemblage of Gill (1970). In addition the chemistry of Clarno rocks is similar to rocks regarded as calc-alkaline by others (Jakes and White, 1972; Chayes, 1969). Hence, although the Clarno rocks are calcic as defined by Peacock (1931) they display many characteristics indicative of calc-alkaline rocks. This is not entirely unexpected; as noted by Miyashiro (1974) continuous gradation exists between the alkalic and non-alkalic series.

As shown by Figure 25 most of the Clarno rocks plot on the boundary between the tholeiitic and high alumina fields of Kuno (1968). This was also found to be the case by Novitsky-Evans (1974).

When the major chemical oxides of individual samples are plotted against their relative position in the

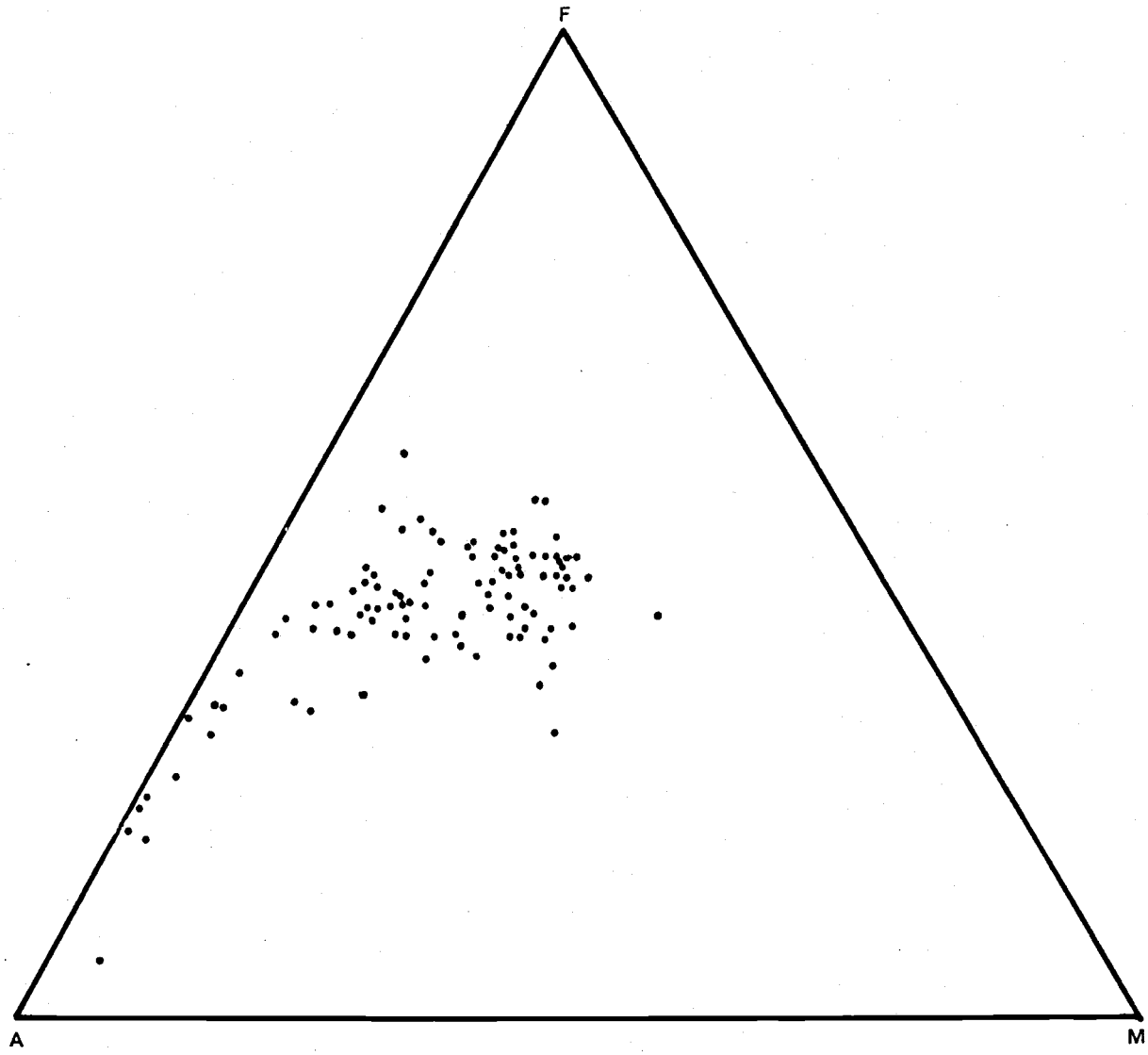

Figure 26 - AFM diagram of Clarno rocks showing low iron enrichment.

Clarno stratigraphic section no definite trends are produced. This was also found to be the case by Barnes (1978).

STRUCTURE

The structural relations displayed by the rocks in the project area are the result of several episodes of deformation which affected this region during Tertiary time. These relations are often difficult to determine because of the nature of the rocks making up the Clarno Group. The Upper Clarno lavas often lack primary bedding features and are thought to have filled canyons and valleys. For this reason the lavas lack the continuity over broad areas displayed by the Lower Clarno units and may have been deposited with large initial dips.

The most significant structural feature of the project area is the east-west trending Mitchell Fault. The fault dips in a vertical direction and has a crush zone up to 250 m wide. Movement along the fault is primarily of a right lateral strike-slip nature. Oles and Enlows (1971), however, suggest that the fault may have experienced dip-slip displacement early in its history prior to the onset of the strike-slip movement. The fault can be traced from the boundary of the project area to the vicinity of Mitchell, 19 km to the east (Oles and Enlows, 1971; Owen, 1977).

Within the project area the fault is inconspicuous; it is not well displayed on aerial photographs as is

the case in the Mitchell Quadrangle (Oles and Enlows, 1971). In the eastern half of the project area the location of the fault is defined by a subtle, but abrupt change in the stratigraphic units across it. North of the fault most of the rocks belong to the Pyroxene Andesite Unit of the Upper Clarno Formation. These andesites have been juxtaposed against the Quartz-bearing Andesite Unit of the Upper Clarno and the andesites of the Heflin Creek Member of the Lower Clarno which are found south of the fault. A small section of the fault in this area is mineralized with cinnabar which was mined intermittently between 1937 and 1943 (Brooks, 1963).

In the western one-half of the project area the location of the fault is not as well defined. If the fault continues on trend from the eastern part of the project area it should displace strata on the southern slopes of Stephenson Mountain. Unfortunately most of the lavas of the Upper Clarno are pyroxene andesites and a fault juxtaposing similar types of lava can be difficult to identify. As shown on Plate 1 the rhyolite flows and glassy andesite dikes adjacent to this trend have not been cut by a fault of major displacement. Hence, it is suggested that the Mitchell Fault is located within the .6 km wide corridor between these units.

Such a proposal is supported by various lines of evidence. Plate 1 shows the location of several pods of glassy andesite which define an east-west trend. All of these pods contain xenoliths of andesite and are extremely brecciated. It is thought that the pods represent pieces of larger intrusions that were emplaced along the fault and then fragmented by it. The andesite flows along this trend often display aberrant attitudes and are oxidized to a dusky red (SR 3/4). In addition there are two other east-west trending strike-slip faults in this area and, as shown by the dikes which they offset, displacement is greater on the fault nearer the proposed trace of the Mitchell Fault.

The amount of strike-slip displacement along the Mitchell Fault has been calculated by different authors using different lithologic units as points of reference. Oles and Enlows (1971) have calculated about 6.7 km of displacement on the basis of offset segments of a basaltic dike located near the town of Mitchell. Taylor (1978, personal communication) has suggested that the segments correlated by Oles and Enlows (1971) are different dikes and that actual displacement is on the order of 4.6 km. His calculation is based on a set of intrusive bodies found in the Mitchell area which he postulated have been displaced by the fault. The data

of this study suggest a strike-slip displacement along the fault on the order of 5 km. This figure is based on offset recorded by the western boundary of the Quartz-bearing Andesite Unit of the Upper Clarno. As shown by Plate 1 the location of this boundary south of the Mitchell Fault has been extrapolated beneath landslide debris and therefore may contain some error. Additional error may have been introduced due to dip-slip movement on the fault or variations in the levels of exposure of the displaced strata.

Two other strike-slip faults have been identified in the area. The faults are located in Sec. 6, T. 11 S., R. 19 E., less than one kilometer south of the Mitchell Fault. They cut the lavas of the Upper Clarno and a group of glassy andesite dikes. As illustrated by displaced segments of the dikes, the faults are right lateral and trend in an east-west direction. The amount of offset recorded by these dikes indicates 50 m of displacement along the southern fault and 200 m of displacement along the northern fault.

Several other faults have been identified in the project area. All of these faults are of limited extent and appear to have displacements ranging from 5 to 30 m. The sense of movement on these faults is indicated on Plate 1.

The strata of the project area record the effects of two major periods of tilting and folding. The earlier period of deformation tilted the Lower Clarno strata of the area along a north-northeast axis. These lavas and sedimentary rocks dip an average of 20° to 30° to the west and probably represent the western limb of a fold which has been mapped to the east by Owen (1977).

The second period of deformation gently tilted both the Upper and Lower Clarno rocks to the north toward the axis of the Sutton Mountain Syncline. The axis of this syncline is found in the northwest corner of the project area and has been traced to the east by Owen (1977), Barnes (1978), Huggins (1978) and Oles and Enlows (1971).

As mentioned earlier in this study a major unconformity forms the basis for the division between the Upper and Lower Clarno Formations. In the Stephenson Mountain area this unconformity is best recorded in Sec. 1, 2, and 12, T. 12 S., R. 19 E. Here the Lower Clarno strata strike approximately N 10° E and dip about 25° to the west. The unconformable Upper Clarno strata to the west have a strike of about N 50° E and dip generally less than 20° to the north. The unconformity is also marked by subtle lithologic changes between the lavas of the two formations as shown in previous

sections of this study. Nowhere in the study area were ancient regoliths identified which could mark the exact location of the hiatus. Therefore the location of the unconformity has been depicted as approximate on Plate 1 and is probably within .3 km of the true location.

GEOLOGIC HISTORY AND CONCLUSIONS

The geologic history of the Stephenson Mountain area extends from Early Tertiary time to the present. During the time period extending from Middle Eocene to Lower Oligocene at least 2,500 m of volcanic and volcanoclastic strata which makes up the Clarno were deposited. These rocks have been subjected to faulting and repeated folding and have been intruded by rocks ranging in composition from andesite to rhyolite. The origin of Clarno volcanism and the subsequent diastrophism is uncertain but may be related to Early Tertiary subduction tectonics.

The earliest event recorded in the project area is the deposition of lacustrine sedimentary rocks of the Ross Flat Member of the Lower Clarno Formation. These rocks are composed primarily of epiclastic sands and silts which, on the basis of paleocurrent indicators, were transported from highlands lying to the southeast (Owen, 1977). As suggested by thin undisturbed beds of very fine grain silt, at least part of the basin was below wave base. Sedimentation along the margins of the lake was less serene; normal sedimentary processes were occasionally interrupted by mudflows and lava flows which reached the area. Near the end of Ross Flat time the Clarno ignimbrite was deposited and before it could

undergo much erosion the lavas of the Heflin Creek Member covered the area. These lavas are the youngest rocks of the Lower Clarno Formation exposed in the area.

The climatic conditions during this time were semi-tropical and vegetation in the area must have been similar to that seen today in the mountains of Costa Rica and Guatemala (Williams, 1948). The Lower Clarno landscape was dominated by gently rolling hills and valleys as indicated by the nearly uniform thickness and distribution of the Clarno Ignimbrite.

Following deposition of the Lower Clarno rocks the strata were subjected to tilting and folding. Oles and Enlows (1971) postulate that these events are the result of an episode of the Laramide Orogeny. Erosion followed this tilting and reduced the Heflin Creek Member to its present thickness.

Events of the Upper Clarno time are the next to be recorded in the project area. The first lavas to be deposited on the eroded surface of the Lower Clarno flows belong to the Quartz-bearing Andesite Unit of the Upper Clarno Formation. As shown by this study these lavas display subtle, but distinct differences when compared to the lavas of the Lower Clarno. Hence, at least in the Stephenson Mountain area the Upper Clarno-Lower Clarno division has both a structural and a litho-

logic basis. Gradually the quartz-bearing andesites of the Upper Clarno gave way to the pyroxene andesites which dominate the formation. Late in Clarno time the rhyolite flows of the Upper Clarno Formation were extruded. These rhyolites filled valleys and gullies eroded into the andesitic terrain and were subsequently buried by younger Clarno pyroxene andesites.

During the span of Upper Clarno deposition many, if not all, of the intrusives of the area were emplaced. The porphyritic andesite intrusions are thought to represent plutonic or subvolcanic phases of the Upper Clarno pyroxene andesite lavas. The glassy andesite intrusions and the rhyolite intrusions were emplaced along zones of weakness in the Upper Clarno lavas.

Concurrent with, or slightly pre-dating these intrusions, movement along the Mitchell Fault commenced. As shown by data from the study area about 5 km of right-lateral displacement along the fault can be demonstrated. Many of the other faults of the area have a trend similar to that of the Mitchell Fault and probably occurred during this time interval.

During Upper or post-Upper Clarno time the strata of the area again underwent a period of folding which produced the beginnings of the Sutton Mountain Syncline.

The history of the remainder of the Tertiary period is not recorded in the rocks of the project area. The

John Day and other Post-Eocene formations of central Oregon may have covered parts of the area. If so, they have since been eroded away. The last events recorded in the project area are those of Quaternary erosion and deposition of alluvium.

The origin of Clarno volcanism has been the subject of much speculation since the advent of plate tectonic theory. Calc-alkaling andesitic lavas similar to those making up the Clarno Group are abundant near subsiding plate margins and it is possible that the Clarno flows were derived by processes resulting from such plate interactions.

Numerous authors (Hamilton, 1969; Hamilton and Meyers, 1966; Atwater, 1970) propose that the oceanic crust of the eastern Pacific was being subducted beneath the North American plate during Early Tertiary time. Rogers and Novitsky-Evans (1977) suggest that a north-south trending subduction zone was active in western Oregon during Early Tertiary time and that it was responsible for Clarno volcanism. Wilson (1973) also considers a north-south trench likely but notes that the K_2O vs. SiO_2 trend seen in rocks east of the proposed trench is not in accord with the expected trend (Dickinson, 1975) seen over benioff zones elsewhere.

Hamilton (1969) and Hamilton and Meyers (1966) have postulated a subduction zone for Early Tertiary time

trending northeast through central Oregon. The serpentine belts of Hess (1937) and the quartz diorite line of Moore (1959) outline such a trend. The position of the Eocene shoreline proposed by Lovell (1969) also lends support to this hypothesis. If a northeast trending trench was active during Early Tertiary time in Oregon, then the Clarno lavas may be its surface manifestations. McWilliams (1977) suggests that between 36 and 40 m.y. ago subduction was initiated along a trench lying west of the present day Oregon coastline. His data imply that, for an undetermined length of time between 20 and 40 m.y. b.p., subduction was occurring simultaneously along both of these trenches. Hence, the volcanics of the Cascade and Clarno areas may be the result of subduction along different trenches and the K_2O discrepancy noted by Wilson (1973) is irrelevant.

Rogers and Novitsky-Evans (1977) note that 23 percent of Clarno rocks contain less than 56 percent SiO_2 and 23 percent contain greater than 63 percent SiO_2. They also observe that Clarno andesites have a low absolute strontium content and that the K_2O vs. SiO_2 plot of Clarno rocks is intermediate between that of continental suites and island arc suites. In addition the andesites of the Clarno Formation contain abundant pyroxenes but are lacking in hornblende and are entirely subaerial. When these facts are compared to the data

of Jakes and White (1972), Rogers and Novitsky-Evans (1977) conclude that Clarno volcanism occurred on a thin continental crust. As noted by Barnes (1978) the observations of Rogers and Novitsky-Evans (1977) are in conflict with the data from this region on one point; the K_2O vs. SiO_2 plot of Clarno rocks is not of an intermediate nature, but compares favorably with the continental suites Rogers and Novitsky-Evans (1977) show. This conclusion is also supported by the data presented in this study.

Rogers and Novitsky-Evans (1977) and Barnes (1978) have applied their data to the K-h diagrams of Hatherton and Dickinson (1969) and propose depths to the benioff zone of 120 km and 170 km respectively. The data presented in this study suggest a depth intermediate between these two limits. The validity of such interpretations, however, has been questioned by Cordie and Potts (1969) who demonstrate that the average potash content in subduction related volcanics increases linearly with increasing crustal thickness. Also, as noted by Nielson and Stoiber (1973), lavas from some volcanic arcs have a lower total potassium content than lavas from other volcanic arcs. Hence, depending on the original potassium content of the magmas and the thickness of the continental crust, the calculated depth to the subduction zone could be in error by a significant amount.

Many other plate tectonic scenarios have been advanced to account for the rocks of central Oregon. It would be well to remember that much detailed field work needs to be done before any of these hypotheses can be considered viable. Also, as noted by Robyn (1977), "Not all calc-alkaline rocks of the interior of the western United States are related to subduction".

BIBLIOGRAPHY

Atwater, T., 1970, Implications of plate tectonics for the Cenozoic tectonic evolution of western North America: Geol. Soc. Amer. Bull., v. 81, p. 3513-3536.

Bagnold, R.A., 1954, Experiments on a gravity-free dispersion of large solid spheres in a Newtonian fluid under sheer: Roy. Soc. London, Proc., Ser. A., v. 225, p. 49-63.

Barnes, T.J., 1978, Geology of the Sand Mountain Area, western Wheeler County, Oregon: Unpublished M.S. Thesis, Oregon State University, 119p.

Bhattachavji, S., 1967, Flowage Differentiation: Science, v. 145, p. 150-153.

Bowen, N.L., 1913, The melting phenomena of plagioclase feldspars: Amer. Jour. of Sci., v. 35, p. 577.

_____, 1928, The evolution of igneous rocks: Princeton University Press, 528p.

Brooks, H.C., 1963, Quicksilver in Oregon: Oregon Dept. Geol. Min. Ind. Bull. 55, p. 163-164.

Calkins, F.C., 1902, A contribution to the petrography of the John Day Basin, Oregon: Calif. Univ. Pub., Dept. Geol. Bull., v. 3, p. 109-172.

Chaney, R.W., 1952, The ancient forests of Oregon: Ore. State System Higher E., Condon Lectures, Eugene, Oregon, p. 56.

Chayes, F., 1969, The chemical composition of Cenozoic andesite; in McBirney, A.R., ed., Proceedings of the andesite conference: Ore. Dept. Geol. Min. Ind., But. 65, p. 1-11.

Condie, K.C., and Potts, M.J., 1969, Calc-alkaline volcanism and the thickness of the early Precambrian crust in North America: Canadian Journal of Earth Sciences, v. 6, p. 1179-1183.

Dickinson, W.R., 1975, Potash-depth (K-h) relations in continental margin and intra-oceanic magmatic arcs: Geology, v. 3, p. 53-56.

Enlows, H.E., and Oles, K.F., 1973, Cretaceous and Cenozoic stratigraphy of north-central Oregon: Clarno group in "Geologic field trips in northern Oregon and southern Washington": Ore. Dept. Geol. Min. Ind. Bull. 77, p. 15-19.

_____, and Parker, D.J., 1972, Geochronology of the Clarno igneous activity in the Mitchell Quadrangle, Wheeler County, Oregon: Ore Bin, v. 34, p. 104-110.

Evernden, J.F., Savage, D.E., Curtis, G.H., and James, G.T., 1964, Potassium-argon dates and the Cenozoic mammalian chronology of North America: Amer. Jour. of Sci. v. 262, p. 145-198.

_____, and James, G.T., 1964, Potassium-argon dates and Tertiary floras of North America: Amer. Jour. of Sci.; v. 262, p. 945-974.

Ewart, Anthony, 1965, Mineralogy and petrogenesis of the Whakamaru ignimbrite in the Maraetai area of the Taupo volcanic zone, New Zealand: New Zealand Jour. of Geol. and Geophys., v. 8, No. 4, p. 611-677.

Fisher, R.V., 1961, Proposed classification of volcaniclastic sediments and rocks: Geol. Soc. Amer. Bull., v. 72, p. 1409-1414.

_____, 1967, Early Tertiary deformation in north-central Oregon: A.A.P.G. Bull., v. 51, No. 1, p. 111-123.

_____, and Mattinson, J.M., 1968, Wheeler Gorge turbidite-conglomerate series, California; inverse grading: Jour. Sedimentary Petrology, v. 38, p. 1013-1023.

Gill, J.B., 1970, Geochemistry of Viti Levu, Fiji, and its evolution as an island arc: Contr. Mineral Petrol., v. 27, p. 179-203.

Goddard, E.N., 1970, Rock-Color Chart: The rock-color chart committee, Geol. Soc. Amer.

Green, T.H., and Ringwood, A.E., 1968a, Genesis of the calc-alkaline igneous rock suite: Contr. Mineral and Petrol., v. 18, p. 105-162.

_____, 1968b, Origin of garnet phenocrysts in calc-alkaline rocks: Contr. Mineral and Petrol., v. 18, p. 163-174.

Gregory, Irene, 1970, An ancient acacia wood from Oregon: Ore Bin, v. 32, No. 11, p. 205-210.

Hamilton, W., 1969, Mesozoic California and the underflow of Pacific mantle: Geol. Soc. Amer. Bull., v. 80, p. 2409-2430.

_____, and Meyers, W.B., 1966, Cenozoic Tectonics of the western United States: Rev. Geophys., v. 4, p. 509-549.

Hanson, Bruce C., 1973, Geology and vertebrate faunas in the type area of the Clarno formation, Oregon: Cord. Sect. Abs. 69th Meeting Geol. Soc. Amer., v. 5, No. 1, p. 87-88.

Hatherton, T. and Dickinson, W.R., 1969, The relationship between andesite volcanism and seismicity in Indonesia, the Lesser Antilles, and other island arcs: Jour. Geophys. Research, v. 74, p. 5301-5310.

Hess, H.H., 1937, Island arcs, gravity anomalies and serpentine intrusions: 17th Internat. Geol. Cong., Moscow, Rept. 17, v. 2, p. 263.

Huggins, J.W., 1978, Geology of a portion of the Painted Hills Quadrangle, Wheeler County, north central Oregon: Unpublished M.S. thesis, Oregon State University, 129p.

Jakes, P., and White, A.J.R., 1972, Major and trace element abundances in volcanic rocks of orogenic areas: Geol. Soc. Amer. Bull., v. 83, p. 29-39.

Knowlton, Frank H., 1902, Fossil flora of the John Day Basin, Oregon: U.S.G.S. Bull., 204, 153p.

Kuno, H., 1950, Petrology of Hadone Volcano and the adjacent areas, Japan: Geol. Soc. Amer. Bull., v. 61, p. 951-1020.

_____, 1968, Differentiation of basalt magmas: in Basalts, v. 2, Interscience, New York, p. 689-736.

Lovell, J.P.B., 1969, Tyee Formation: Undeformed turbidites and their lateral equivalents: Mineral. and paleogeog.: Geol. Soc. Amer. Bull., v. 80, p. 9-22.

Lukanuski, J.N., 1963, Geology of part of the Mitchell Quadrangle, Jefferson and Crook Counties, Oregon: Unpublished M.S. thesis, Oregon State University, 90p.

McKee, Thomas M., 1970, Preliminary report on fossils, fruits and seeds from the Mammal Quarry of the Clarno Formation, Oregon: Ore Bin, v. 32, No. 7, p. 117-132.

McWilliams, R.G., 1978, Early tertiary rifting in western Oregon-Washington: Amer. Assoc. Pet. Geol., v. 62, No. 7, p. 1193-1197.

Merriam, J.C., 1901, A contribution to the geology of the John Day Basin: California University Pub., Dept. of Geol. Bull., v. 2, No. 9, p. 269-314.

Miyashuro, Akiho, 1974, Volcanic rock series in island arcs and active continental margins: Amer. Jour. of Sci., v. 274, p. 321-355.

Moore, J.G., 1959, The quartz diorite boundary line in the western United States: Jour. of Geol., v. 67, p. 198-210.

Moorhouse, W.W., 1959, The study of rocks in thinsection: Harper Book Co., New York, 514 p.

Nicholls, S.R., Carmichael, I.S.E., and Stormer, J.C., 1971, Silica activity and P total in igneous rocks: Contri. Mineral. and Petrol., v. 33, p. 1-20.

Nielson, D.R., and Stoiber, R.E., 1973, Relationship of potassium content in andesitic lavas and depth to the seismic zone: Jour. Geophys. Res., v. 78, p. 6887-6892.

Novitsky-Evans, J.M., 1974, Petrochemical study of the Clarno Group: Eocene-Oligocene continental margin volcanism of north-central Oregon, M.A. thesis, Rice Univ., Houston, Texas, p. 97.

Oles, K.F. and Enlows, H.E., 1971, Bedrock geology of the Mitchell Quadrangle Wheeler County, Oregon: Ore. Dept. Geo. Min. Ind. Bull., 72, 62p.

Owen, P., 1977, An examination of the Clarno Formation in the vicinity of the Mitchell Fault, Lawson Mountain and Stephenson Mountain area, Jefferson and Wheeler Counties: Unpublished M.S. thesis, Oregon State University, 166p.

Peacock, M.A., 1931, Classification of igneous rock series: Jour. of Geol. v. 39, No. 1, p. 54-67.

Peck, D.L., 1964, Geologic reconnaissance of the Antelope-Ashwood area, north-central Oregon: U.S. Geol. Survey, Bull., 1161-D, p. 1-26.

Robinson, P.T., 1976, Reconnaissance geologic map of the John Day Formation in the southwestern part of the Blue Mountains and adjacent areas: U.S. Geol. Survey Misc. Invest. Map I-872.

Robyn, T.L., 1977, Origin of a calc-alkaline volcanic suite, NE Oregon: Geol. Soc. Amer. Programs with Abs., v. 9, No. 7, p. 1145-1146.

Ross, C.S., and Smith, R.L., 1961, Ash-flow tuffs: their origin, geologic relations, and identification: U.S. Geol. Survey Prof. Papper 366, p. 2-8.

Rittman, A., 1962, Volcanoes and their activity: John Wiley, New York, 312p.

Rogers, J.J.W., and Novitsky-Evans, Joyce M., 1977, The Clarno Formation of central Oregon, U.S.A. - Volcanism on a thin continental margin: Earth and Planetary Science Letters, v. 34, p. 55-66.

Schmincke, Hans-Ulrich, 1967, Graded lahars in the type section of the Ellensburg Formation, south-central Washington: Jour. Sedimentary Petrology, v. 37, p. 438-448.

Scott, R.A., 1954, Fossil fruits and seeds from Eocene Clarno Formation of Oregon: Paleontolographica, 96b, p. 66-97.

Steiner, A., 1963, Crystallization behavior and origin of acid ignimbrite and rhyolite magma in the North Island of New Zealand: Bull. Volcanol., v. 25, p. 217-241.

Stirton, R.A., 1944, A rhinoceros tooth from the Clarno Eocene of Oregon: Jour. Paleon. v. 18, p. 265-267.

Swanson, D.A., 1969, Reconnaissance geologic map of the east half of Bend Quadrangle, Crook, Wheeler, Jefferson, Wasco and Deschutes Counties, Oregon: U.S.G.S. Map I-568.

_____, and Robinson, P.T., 1968, Base of the John Day Formation in and near the Horse Heaven Mining District, north-central Oregon: U.S.G.S. Professional Paper 600D, p. D154-D161.

Taylor, E.M., 1978, Field Geology of S.W. Broken Top Quadrangle, Oregon: Ore. Dept. Geo. Min. Ind. Bull., Special Paper 2.

_____, 1978, Personal communication.

_____, 1979, Personal communication.

Tobi, A.C., 1963, Plagioclase determination with the aid of the extinction angles in sections normal to (010). A critical comparison of current Albite-Carlsbad charts: Amer. Jour. Sci., v. 261, p. 157-167.

Tuttle, O.F., and Bowen, N.L., 1958, Origin of granite in the light of experimental studies in the system $NaAlSi_3O_8$ - $KAlSi_3O_8$ - SiO_2 - H_2O: Geol. Soc. Amer. Mem., No. 74.

Vance, J.A., 1962, Zoning in igneous plagioclase: normal and oscillatory zoning: Amer. Jour. Sci., v. 260, p. 746-760.

_____, 1965, Zoning in igneous plagioclase and patchy zoning: Jour. Geol., v. 73, p. 636-651.

Waters, A.C., Brown, R.E., Compton, R.R., Staples, L.W., Walker, G.W., and Williams, H., 1951, Quicksilver deposits of the Horse Heaven Mining District, Oregon: U.S.G.S. Bull., 969-E, p. 105-149.

Wilkinson, W.D., and Oles, K.F., 1968, Stratigraphy and paleoenvironments of Cretaceous rocks, Mitchell Quadrangle, Oregon: Amer. Assoc. Petrol. Geol. Bull., v. 52, p. 129-161.

Wilson, P.M., 1973, Petrology of the Cenozoic volcanic rocks of the basal Clarno Formation, central Oregon: Unpublished M.A. thesis, Rice University, Houston, Texas, 47p.

Williams, Howell, 1948, The ancient volcanoes of Oregon: Ore. Supt. of Higher Education, p. 1-64.

Wright, F.E., and Larsen, E.S., 1909, Quartz as a geologic thermometer: Amer. Jour. of Sci., v. 27, p. 421-440.

APPENDICES

Appendix A. Chemical Analyses of Clarno Rocks. (Oxides tabulated are in weight percent) Sources: JWH - Huggins (1978); TB - Barnes (1978); HS - this study.

Sample	JWH-2	JWH-6	JWH-7	JWH-10	JWH-13	JWH-14
SiO_2	66.2	64.3	63.3	62.0	59.0	57.5
Al_2O_3	16.8	16.1	16.2	17.7	16.9	17.0
FeO	4.5	5.6	5.9	5.1	6.8	7.7
CaO	3.5	5.2	5.1	6.0	6.8	6.8
MgO	0.5	2.9	2.0	1.1	3.5	3.9
K_2O	3.00	1.80	1.75	1.65	1.05	1.00
NaO_2	3.7	4.1	3.8	4.1	3.9	3.8
TiO_2	0.75	0.80	1.00	0.80	1.00	1.00
Total	98.95	100.80	99.05	98.45	99.15	98.70

JWH-2 Dacite: elevation 1,800 ft., NE$\frac{1}{4}$, SE$\frac{1}{4}$, Sec. 1, T. 10 S., R. 20 E.

JWH-6 Dacite: elevation 2,000 ft., middle Sec. 1, T. 10 S., R. 20 E.

JWH-7 Porphyritic two-pyroxene bearing dacite: elevation 2,400 ft., middle SW$\frac{1}{4}$, Sec. 1, T. 10 S., R. 20E.

JWH-10 Andesite: elevation 1,720 ft., SE$\frac{1}{4}$, NE$\frac{1}{4}$, Sec. 1, T. 10 S., R. 20 E.

JWH-13 Two-pyroxene bearing andesite: elevation 1,560 ft., NE$\frac{1}{4}$, NE$\frac{1}{4}$, Sec. 2, T. 10 S., R. 20 E.

JWH-14 Two-pyroxene bearing basaltic andesite: elevation 1,560 ft., NE$\frac{1}{4}$, NW$\frac{1}{4}$, Sec. 2, T. 10 S., R. 20 E.

Sample	JWH-15A	JWH-15B	JWH-16	JWH-17	JWH-18	JWH-38
SiO_2	58.2	65.2	65.2	63.9	64.3	58.7
Al_2O_3	16.3	16.4	16.0	15.9	16.0	16.8
FeO	8.1	4.8	5.1	5.3	5.3	7.2
CaO	6.4	4.8	4.9	5.2	5.2	8.0
MgO	3.3	1.3	2.1	2.0	2.0	3.5
K_2O	1.25	1.90	1.90	1.80	1.80	0.80
Na_2O	4.0	4.3	4.1	4.3	3.9	3.1
TiO_2	1.30	0.75	0.70	0.80	0.75	1.20
Total	98.85	99.45	100.00	99.20	99.25	99.30

JWH-15A Two-pyroxene bearing andesite: elevation 1,600 ft., middle Sec. 2, T. 10 S., R. 20 E.

JWH-15B Porphyritic two-pyroxene bearing dacite: elevation 2,000 ft., NW¼, SE¼, Sec. 2, T. 10 S., R. 20 E.

JWH-16 Porphyritic two-pyroxene bearing dacite: elevation 2,100 ft., NW¼, SE¼, Sec. 2, T. 10 S., R. 20 E.

JWH-17 Augite bearing dacite: elevation 2,200 ft., NW¼, SE¼, Sec. 2, T. 10 S., R. 20 E.

JWH-18 Porphyritic two-pyroxene bearing dacite: elevation 2,360 ft., NW¼, SE¼, Sec. 2, T. 10 S., R. 20 E.

JWH-38 Quartz bearing andesite: elevation 1,950 ft., SW¼, NE¼, Sec. 11, T. 10 S., R. 20 E.

Sample	JWH-39	JWH-40	JWH-41	JWH-46	JWH-49	JWH-50
SiO_2	56.3	64.5	57.5	64.6	64.9	63.3
Al_2O_3	18.0	15.8	18.0	16.3	16.3	16.7
FeO	7.3	5.5	7.3	5.7	5.5	5.7
CaO	7.8	4.4	7.5	4.7	4.6	5.0
MgO	4.5	1.7	4.3	1.6	1.5	1.7
K_2O	0.65	1.90	0.95	1.95	1.85	2.30
Na_2O	4.0	4.3	3.7	4.4	4.5	3.8
TiO_2	1.10	1.00	1.10	1.00	1.00	1.00
Total	99.65	99.10	100.35	100.25	100.15	99.50

JWH-39 Porphyritic two-pyroxene bearing basaltic andesite: elevation 2,000 ft., NE$\frac{1}{4}$, SE$\frac{1}{4}$, Sec. 11, T. 10 S., R. 20 E.

JWH-40 Porphyritic two-pyroxene bearing dacite: elevation 2,100 ft., NE$\frac{1}{4}$, SE$\frac{1}{4}$, Sec. 11, T. 10 S., R. 20 E.

JWH-41 Porphyritic two-pyroxene bearing andesite: elevation 2,140 ft., NE$\frac{1}{4}$, SE$\frac{1}{4}$, Sec. 11, T. 10 S., R. 20 E.

JWH-46 Porphyritic two-pyroxene bearing dacite: elevation 2,120 ft., SW$\frac{1}{4}$, SE$\frac{1}{4}$, Sec. 1, T. 10 S., R. 20 E.

JWH-49 Porphyritic two-pyroxene bearing dacite: elevation 2,320 ft., SW$\frac{1}{4}$, NW$\frac{1}{4}$, Sec. 12, T. 10 S., R. 20 E.

JWH-50 Porphyritic two-pyroxene bearing dacite: elevation 2,360 ft., SW$\frac{1}{4}$, NW$\frac{1}{4}$, Sec. 12, T. 10 S., R. 20 E.

Sample	JWH-52	JWH-56	JWH-64	JWH-68	JWH-70	JWH-72
SiO_2	64.2	64.2	57.2	63.3	56.9	60.5
Al_2O_3	16.8	17.2	16.8	15.9	17.5	15.7
FeO	4.0	5.5	8.7	5.2	7.3	5.8
CaO	5.2	5.0	8.1	5.4	7.4	6.0
MgO	1.8	1.5	3.5	3.2	4.5	3.8
K_2O	1.80	1.65	0.80	1.60	0.95	1.55
Na_2O	4.5	4.6	3.5	4.1	4.0	3.9
TiO_2	0.70	1.00	1.20	0.70	1.05	0.75
Total	99.00	100.65	99.80	99.40	99.60	98.00

JWH-52 Porphyritic quartz bearing dacite: elevation 2,200 ft., NE$\frac{1}{4}$, SE$\frac{1}{4}$, Sec. 11, T. 10 S., R. 20 E.

JWH-56 Porphyritic two-pyroxene bearing dacite: elevation 1,880 ft., SE$\frac{1}{4}$, NW$\frac{1}{4}$, Sec. 13, T. 10 S., R. 20 E.

JWH-64 Basaltic andesite: elevation 1,840 ft., SW$\frac{1}{4}$, SE$\frac{1}{4}$, Sec. 11, T. 10 S., R. 20 E.

JWH-68 Porphyritic quartz bearing dacite: elevation 2,100 ft., center Sec. 14, T. 10 S., R. 20 E.

JWH-70 Porphyritic two-pyroxene bearing basaltic andesite: elevation 2,450 ft., NW$\frac{1}{4}$, SW$\frac{1}{4}$, Sec. 14, T. 10 S., R. 20 E.

JWH-72 Porphyritic quartz bearing andesite: elevation 2,000 ft., NW$\frac{1}{4}$, SW$\frac{1}{4}$, Sec. 3, T. 10 S., R. 20 E.

Sample	JWH-73	JWH-74	JWH-76	JWH-77	JWH-78	JWH-80
SiO_2	59.3	58.0	55.1	59.3	58.5	58.0
Al_2O_3	15.8	16.8	14.9	15.9	16.8	16.9
FeO	6.2	4.9	7.6	5.3	7.4	7.4
CaO	6.1	7.0	8.9	6.1	8.1	7.9
MgO	4.3	4.2	6.7	4.5	3.9	3.7
K_2O	1.35	1.50	0.90	1.25	0.70	1.00
Na_2O	3.9	3.6	3.2	3.8	3.6	3.8
TiO_2	0.80	0.85	0.95	0.85	1.00	1.00
Total	97.75	96.85	98.25	97.00	100.00	99.70

JWH-73 Porphyritic quartz bearing andesite: elevation 2,050 ft., SW¼, SW¼, Sec. 3, T. 10 S., R. 20 E.

JWH-74 Porphyritic quartz bearing andesite: elevation 2,350 ft., NE¼, NE¼, Sec. 9, T. 10 S., R. 20 E.

JWH-76 Two-pyroxene basaltic andesite dike: elevation 1,900 ft., SW¼, SE¼, Sec., 3 T. 10 S., R. 20 E.

JWH-77 Porphyritic quartz bearing andesite: elevation 1,900 ft., SW¼, SE¼, Sec. 3, T. 10 S., R. 20 E.

JWH-78 Porphyritic two-pyroxene bearing andesite: elevation 1,850 ft., SW¼, SE¼, Sec. 3, T. 10 S., R. 20 E.

JWH-80 Porphyritic two-pyroxene bearing andesite: elevation 1,800 ft., SW¼, NW¼, Sec. 3, T. 10 S., R. 20 E.

Sample	JWH-81	JWH-83	JWH-86	JWH-90	JWH-91	JWH-93
SiO_2	60.8	56.7	61.2	55.0	56.7	58.8
Al_2O_3	15.4	16.9	16.1	16.1	15.9	17.6
FeO	6.5	7.7	6.0	8.7	6.9	6.4
CaO	6.0	6.7	5.9	7.5	7.6	7.0
MgO	3.8	3.5	3.9	4.7	5.1	4.1
K_2O	1.60	1.00	1.45	0.75	1.50	1.55
Na_2O	4.0	4.0	3.8	4.3	3.7	3.7
TiO_2	0.80	1.00	0.75	1.15	0.90	0.90
Total	98.90	97.50	99.10	98.20	98.30	100.05

JWH-81 Andesite: elevation 1,540 ft., NE¼, NW¼, Sec. 3, T. 10 S., R. 20 E.

JWH-83 Porphyritic two-pyroxene bearing basaltic andesite: elevation 1,560 ft., NW¼, NE¼, Sec. 3, T. 10 S., R. 20 E.

JWH-86 Porphyritic hypersthene and quartz bearing andesite: elevation 1,840 ft., SE¼, NE¼, Sec. 4, T. 10 S., R. 20 E.

JWH-90 Porphyritic two-pyroxene bearing basaltic andesite: elevation 2,600 ft., SW¼, NW¼, Sec. 9, T. 10 S., R. 20 E.

JWH-91 Porphyritic basaltic andesite: elevation 2,800 ft., NW¼, SW¼, Sec. 9, T. 10 S., R. 20 E.

JWH-93 Porphyritic augite and quartz bearing andesite: elevation 2,750 ft., SW¼, NE¼, Sec. 9, T. 10 S., R. 20 E.

Sample	JWH-99	JWH-100	JWH-102	JWH-103	JWH-105	JWH-110
SiO_2	65.8	62.4	61.7	60.5	61.3	60.0
Al_2O_3	16.4	16.4	16.4	17.4	16.2	17.7
FeO	3.5	6.0	5.2	5.9	5.7	4.2
CaO	4.3	5.2	5.6	6.0	5.4	7.0
MgO	1.3	3.0	2.8	2.3	1.9	4.3
K_2O	1.95	2.05	1.60	1.40	1.75	1.10
Na_2O	4.6	3.7	3.9	4.5	4.3	3.9
TiO_2	0.85	0.70	0.90	1.15	0.80	1.10
Total	98.70	99.45	98.10	99.15	97.35	99.30

JWH-99 Porphyritic hypersthene bearing dacite: elevation 2,400 ft., NE$\frac{1}{4}$, SW$\frac{1}{4}$, Sec. 10, T. 10 S., R. 20 E.

JWH-100 Porphyritic quartz and augite bearing andesite: elevation 2,400 ft., NE$\frac{1}{4}$, SE$\frac{1}{4}$, Sec. 9, T. 10 S., R. 20 E.

JWH-102 Porphyritic two-pyroxene bearing andesite: elevation 3,100 ft., NE$\frac{1}{4}$, NW$\frac{1}{4}$, Sec. 16, T. 10 S., R. 20 E.

JWH-103 Porphyritic hypersthene bearing andesite: elevation 3,100 ft., SE$\frac{1}{4}$, NE$\frac{1}{4}$, Sec. 16, T. 10 S., R. 20 E.

JWH-105 Epidote bearing andesite: elevation 1,800 ft., NW$\frac{1}{4}$, SW$\frac{1}{4}$, Sec. 11, T. 10 S., R. 20 E.

JWH-110 Porphyritic two-pyroxene bearing andesite: elevation 2,800 ft., SE$\frac{1}{4}$, SE$\frac{1}{4}$, Sec. 15, T. 10 S., R. 20 E.

Sample	JWH-113	JWH-119	JWH-123	JWH-134	JWH-138	JWH-140
SiO_2	56.4	57.9	60.5	57.8	57.5	62.5
Al_2O_3	17.3	17.3	17.2	17.8	16.8	15.5
FeO	7.6	8.2	6.0	6.1	7.6	7.8
CaO	7.5	6.6	6.2	7.5	7.0	4.7
MgO	4.3	3.9	2.8	4.3	4.6	1.7
K_2O	1.00	1.00	0.65	1.00	1.00	2.20
Na_2O	3.7	4.3	4.2	4.0	3.8	3.7
TiO_2	1.10	1.40	1.15	1.10	1.05	1.10
Total	98.90	100.60	98.70	99.60	99.35	99.20

JWH-113 Porphyritic two-pyroxene bearing basaltic andesite: elevation 2,200 ft., NE¼, NE¼, Sec. 15, T. 10 S., R. 20 E.

JWH-119 Porphyritic augite and quartz bearing basaltic andesite: elevation 2,760 ft., SW¼, SE¼, Sec. 21, T. 10 S., R. 20 E.

JWH-123 Porphyritic two-pyroxene bearing andesite: elevation 3,000 ft., NE¼, SE¼, Sec. 21, T. 10 S., R. 20 E.

JWH-134 Porphyritic two-pyroxene bearing basaltic andesite: elevation 3,100 ft., SE¼, SW¼, Sec. 21, T. 10 S., R. 20 E.

JWH-138 Porphyritic two-pyroxene bearing basaltic andesite: elevation 2,800 ft., SW¼, NW¼, Sec. 28, T. 10 S., R. 20 E.

JWH-140 Porphyritic two-pyroxene bearing andesite: elevation 2,960 ft., SE¼, NW¼, Sec. 28, T. 10 S., R. 20 E.

Sample	JWH-141	JWH-147	JWH-148	JWH-152	JWH-159	JWH-163
SiO_2	56.5	64.5	65.0	56.8	60.8	65.5
Al_2O_3	17.2	15.8	16.4	16.5	16.2	15.8
FeO	7.7	5.7	4.8	7.9	6.4	5.0
CaO	7.1	4.8	4.0	8.1	6.4	4.2
MgO	4.6	1.7	1.3	5.0	4.1	0.9
K_2O	0.95	1.85	1.90	0.85	1.30	2.15
Na_2O	3.9	3.9	4.3	3.6	3.9	4.5
TiO_2	1.10	1.00	1.00	1.25	0.85	0.85
Total	99.05	99.25	98.70	100.00	99.95	98.90

JWH-141 Porphyritic two-pyroxene bearing basaltic andesite: elevation 3,180 ft., NW¼, SW¼, Sec. 28, T. 10 S., R. 20 E.

JWH-147 Porphyritic two-pyroxene bearing dacite: elevation 2,700 ft., NE¼, SE¼, Sec. 28, T. 10 S., R. 20 E.

JWH-148 Porphyritic augite bearing dacite: elevation 2,650 ft., NE¼, SE¼, Sec. 28, T. 10 S., R. 20 E.

JWH-152 Porphyritic quartz bearing basaltic andesite: elevation 1,760 ft., NW¼, SE¼, Sec. 11, T. 10 S., R. 20 E.

JWH-159 Porphyritic two-pyroxene bearing andesite: elevation 3,600 ft., SE¼, NE¼, Sec. 32, T. 10 S., R. 20 E.

JWH-163 Porphyritic augite bearing dacite: elevation 2,850 ft., NW¼, NW¼, Sec. 34, T. 10 S., R. 20 E.

Sample	JWH-166	JWH-167	JWH-174	JWH-184	JWH-186	JWH-187
SiO_2	64.6	70.0*	61.6	59.2	71.3**	67.5
Al_2O_3	16.0	14.0	15.5	17.6	14.0	16.1
FeO	5.2	3.8	8.0	6.8	3.8	4.4
CaO	4.9	2.2	5.4	6.5	2.2	2.2
MgO	2.4	0.2	2.1	3.3	0.4	0.4
K_2O	1.75	3.08	1.70	1.20	3.20	3.90
Na_2O	3.9	4.8	4.1	3.9	4.4	3.9
TiO_2	0.85	0.60	1.45	1.05	0.50	0.50
Total	99.60	98.65	99.85	99.55	99.85	98.90

JWH-166 Porphyritic two-pyroxene bearing dacite: elevation 3,600 ft., SW¼, SW¼, Sec. 33, T. 10 S., R. 20 E.

JWH-167 Rhyodacite: elevation 3,400 ft., SW¼, SW¼, Sec. 33, T. 10 S., R. 20 E.

JWH-174 Porphyritic two-pyroxene bearing andesite: elevation 2,360 ft., NW¼, SW¼, Sec. 23, T. 10 S., R. 20 E.

JWH-184 Porphyritic two-pyroxene bearing andesite: elevation 1,820 ft., SW¼, NW¼, Sec. 25, T. 10 S., R. 20 E.

JWH-186 Porphyritic pyroxene bearing dacite: elevation 2,000 ft., NE¼, NE¼, Sec. 35, T. 10 S., R. 20 E.

JWH-187 Porphyritic pyroxene bearing dacite: elevation 2,200 ft., NW¼, SW¼, Sec. 36, T. 10 S., R. 20 E.

* minor secondary quartz
** large amounts of secondary quartz - should be similar to JWH-187

Sample	TB21	TB31	TB33	TB35	TB36	TB37
SiO_2	59.2	69.2	74.2	63.0	63.7	55.8
Al_2O_3	16.9	15.1	13.8	16.7	16.6	18.0
FeO	6.7	3.3	1.8	5.5	6.0	8.1
MgO	3.6	0.3	0.2	1.8	1.6	3.7
CaO	6.4	2.6	0.5	5.0	5.2	7.3
Na_2O	4.0	4.2	2.2	4.1	4.1	3.8
K_2O	1.25	3.05	5.05	1.50	1.65	1.45
TiO_2	1.00	0.40	0.15	0.85	0.90	1.35
Total	99.15	98.25	97.90	98.55	99.85	99.50

TB21 On top of knob, elevation 3,040 ft., NE$\frac{1}{4}$ of SE$\frac{1}{4}$ of Sec. 17, T. 11 S., R. 21 E.; augite-bearing andesite.

TB31 Southeast of Sand Mountain summit, elevation 3,500 ft., NW$\frac{1}{4}$ of SE$\frac{1}{4}$ of Sec. 18, T. 11 S., R. 21 E.; vesicular rhyodacite.

TB33 Immediately east of saddle, elevation 3,100 ft., Sec. 13, T. 11 S., R. 20 E.; vesicular, flow-banded rhyolite.

TB35 On northwest end of ridge, elevation 3,260 ft., W$\frac{1}{2}$ of SW$\frac{1}{4}$ of Sec. 18, T. 11 S., R. 21 E.; glomeroporphyritic andesite.

TB36 On southeast side of ridge, elevation 3,160 ft., SW$\frac{1}{4}$ of SW$\frac{1}{4}$ of Sec. 18, T. 11 S., R. 21 E.; porphyritic dacite.

TB37 On knob on ridge, elevation 3,160 ft., W$\frac{1}{2}$ of SW$\frac{1}{4}$ of Sec. 17, T. 11 S., R. 21 E.; porphyritic basaltic andesite.

Sample	TB49	TB50	TB55	TB42	TB45	TB47
SiO_2	66.2	74.5	62.5	60.0	57.7	72.0
Al_2O_3	16.5	14.7	16.2	16.4	17.1	15.5
FeO	4.5	3.1	6.3	7.4	7.8	2.6
MgO	1.3	0.1	1.4	2.5	3.1	0.1
CaO	4.4	1.9	5.0	5.8	4.0	1.6
Na_2O	4.1	4.5	4.3	4.2	2.8	3.7
K_2O	2.60	3.50	1.70	1.55	5.70	4.20
TiO_2	0.75	0.25	1.05	1.55	1.10	0.35
Total	100.45	102.65	98.55	98.40	99.30	100.15

TB49 On west side of hill "2732", elevation 2,700 ft., S$\frac{1}{2}$ of Sec. 10, T. 11 S., R. 20 E.; dacite.

TB50 West side of southernmost knob in row of three, elevation 2,720 ft., SW$\frac{1}{4}$ of NW$\frac{1}{4}$ of Sec. 10, T. 11 S., R. 20 E.; flow-banded-brecciated rhyodacite.

TB55 On knob on ridge, elevation 2,680 ft., NW$\frac{1}{4}$ of SW$\frac{1}{4}$ of Sec. 9, T. 11 S., R. 20 E.; glomeroporphyritic augite-bearing andesite.

TB42 On northwest end of ridge, elevation 2,980 ft., SW$\frac{1}{4}$ of NW$\frac{1}{4}$ of Sec. 13, T. 11 S., R. 20 E.; porphyritic andesite.

TB45 Knob immediately north of road, elevation 2,680 ft., Sec. 14, T. 11 S., R. 20 E.; basaltic andesite (dike rock).

TB47 On knob, elevation 2,280 ft., NE$\frac{1}{4}$ of SE$\frac{1}{4}$ of Sec. 2, T. 11 S., R. 20 E.; flow-banded rhyodacite.

Sample	TB03	TB04	TB10	TB11	TB38	TB39
SiO_2	58.5	58.0	57.9	57.0	57.2	54.8
Al_2O_3	16.2	16.1	16.7	17.3	17.0	18.7
FeO	9.0	8.9	8.3	7.7	8.5	7.7
MgO	3.7	3.1	3.3	3.3	3.1	3.9
CaO	6.2	5.2	6.6	6.6	6.7	7.6
Na_2O	4.2	3.2	3.8	3.8	3.8	3.8
K_2O	1.20	3.30	1.25	1.55	1.45	1.40
TiO_2	1.20	1.15	1.25	1.20	1.20	1.30
Total	100.20	99.15	99.10	98.55	99.05	99.20

TB03 Top of hill, elevation 3,200 ft., SW¼ of Sec. 8, T. 11 S., R. 21 E.; porphyritic augite-bearing andesite.

TB04 Elevation 2,380 ft., on ridge, NE¼ of NW¼ of Sec. 8, T. 11 S., R. 21 E.; augite-bearing basaltic andesite.

TB10 Top knob at elevation 2,840 ft., NW¼ of NE¼ of Sec. 7, T. 11 S., R. 21 E.; augite-bearing basaltic andesite.

TB11 On ridge next to prominent drainage, elevation 2,480 ft., SW¼ of SE¼ of Sec. 6, T. 11 S., R. 21 E.; Augite-bearing basaltic andesite.

TB38 On prominent ridge, elevation 2,220 ft., E½ of NE¼ of Sec. 8, T. 11 S., R. 21 E.; augite-bearing basaltic andesite.

TB39 In gully at elevation 3,080 ft., SW¼ of SE¼ of Sec. 18, T. 11 S., R. 21 E.; porphyritic basaltic andesite.

Sample	TB57	TB58	TB59	TB60	TB61	TB62
SiO_2	64.4	64.0	65.5	60.9	63.7	68.3
Al_2O_3	15.7	15.9	15.8	17.1	15.4	15.3
FeO	6.1	5.5	5.1	6.5	7.2	4.7
MgO	1.2	2.0	0.9	2.2	1.2	0.5
CaO	4.4	4.9	4.1	5.7	4.6	3.6
Na_2O	3.8	3.8	4.1	4.0	4.1	3.9
K_2O	2.15	1.75	2.10	1.45	1.85	2.20
TiO_2	0.90	0.95	0.90	1.25	1.05	0.90
Total	98.75	98.90	98.50	99.10	99.10	99.40

TB57 On knob on top of prominent ridge, elevation 3,040 ft., E½ of NW¼ of Sec. 8, T. 11 S., R. 20 E.; glomeroporphyritic augite-bearing dacite.

TB58 On ridge, elevation 2,860 ft., SE¼ of NW¼ of Sec. 17, T. 11 S., R. 20 E.; porphyritic augite-bearing dacite.

TB59 On top of hill "3016", Sec. 17, T. 11 S., R. 20 E.; porphyritic augite-bearing dacite.

TB60 On top of knob, elevation 2,560 ft., SE¼ of SE¼ of Sec. 17, T. 11 S., R. 20 E.; porphyritic andesite.

TB61 On small knob, elevation 2,880 ft., NW¼ of SW¼ of Sec. 4, T. 11 S., R. 20 E.; dacite.

TB62 On end of ridge, north of bend in road, elevation 2,360 ft., Sec. 9, T. 11 S., R. 20 E.; porphyritic augite-bearing dacite (?).

Sample	TB14	TB15	TB19	TB20	TB63	TB65
SiO_2	71.5	64.4	58.8	67.0	55.4	64.5
Al_2O_3	14.6	16.5	16.4	16.2	18.2	15.9
FeO	2.7	4.3	8.0	4.0	7.3	4.8
MgO	0.3	1.8	3.4	0.7	4.1	1.2
CaO	1.0	4.6	6.2	3.4	7.7	4.4
Na_2O	3.4	4.3	4.1	4.6	3.3	3.8
K_2O	4.25	1.60	1.25	1.95	0.95	2.10
TiO_2	0.25	0.70	1.60	0.60	1.10	0.85
Total	98.00	98.20	99.85	98.45	98.15	97.65

TB14 Next to bump on ridge, elevation 2,360 ft., SE$\frac{1}{4}$ of NE$\frac{1}{4}$ of Sec. 8, T. 11 S., R. 21 E.; flow-banded rhyodacite.

TB15 In main drainage, elevation 2,300 ft., E$\frac{1}{2}$ of SE$\frac{1}{4}$ of Sec. 8, T. 11 S., R. 21 E.; porphyritic augite-bearing dacite.

TB19 On knob "3050" on boundary between Sections 16 and 17, T. 11 S., R. 21 E.; andesite.

TB20 On top of knob, elevation 3,040 ft., SE$\frac{1}{4}$ of NE$\frac{1}{4}$ of Sec. 17, T. 11 S., R. 21 E.; andesite.

TB63 On knob on ridge, elevation 3,294 ft., SE$\frac{1}{4}$ of NW$\frac{1}{4}$ of Sec. 5, T. 11 S., R. 20 E.; porphyritic hypersthene-bearing basaltic andesite.

TB65 On south side of hill "2812", elevation 2,760 ft., Sec. 3, T. 11 S., R. 20 E.; porphyritic pyroxene-bearing dacite.

Sample	TB68	TB69	HS7859	HS7811	HS7845	HS7823
SiO_2	65.0	71.5	62.6	74.8	60.0	60.5
Al_2O_3	16.1	15.4	16.5	13.9	16.6	16.2
FeO	5.0	1.8	5.5	0.1	6.1	6.3
MgO	0.8	---	2.6	0.4	4.0	3.0
CaO	4.3	2.3	5.3	0.9	6.1	6.1
Na_2O	4.1	4.3	5.0	4.7	4.0	4.2
K_2O	2.20	3.05	1.15	4.20	1.45	0.90
TiO_2	0.90	0.45	0.75	0.10	1.05	0.95
Total	99.40	98.80	99.40	99.70	98.40	99.45

TB68 On knob at end of ridge, elevation 2,320 ft., NW¼ of SE¼ of Sec. 3, T. 11 S., R. 20 E.; porphyritic chlorite-bearing dacite.

TB69 On westernmost of three elongate ridges, elevation 2,180 ft., NW¼ of NW¼ of Sec. 2, T. 11 S., R. 20 E.; flow-banded rhyodacite.

HS7859 Elevation 4,540 ft., SW¼, NW¼, Sec. 18, T. 12 S., R. 20 E.; glassy andesite dike.

HS7811 Elevation 5,010 ft., NW¼, SW¼, Sec. 33, T. 11 S., R. 19 E.; flow-banded rhyolite; rhyolite flows of Upper Clarno Formation.

HS7845 Elevation 3,500 ft., NE¼, SE¼, Sec. 34, T. 11 S., R. 19 E.; porphyritic pyroxene andesite; Pyroxene Andesite Unit of Upper Clarno Formation.

HS7823 Elevation 4,280 ft., SE¼, SE¼, Sec. 1, T. 12 S., R. 19 E.; porphyritic pyroxene andesite; Heflin Creek Member of Lower Clarno Formation.

Sample	HS7892	HS7888	HS7861	HS78327	HS78321	HS7887
SiO_2	60.5	60.5	59.2	61.8	60.9	65.0
Al_2O_3	16.2	17.0	17.3	16.5	16.8	15.5
FeO	6.3	6.3	8.0	6.4	6.3	5.9
MgO	3.8	3.0	4.2	1.4	1.4	1.0
CaO	6.8	6.4	7.6	5.3	5.4	4.0
Na_2O	3.7	4.0	4.3	4.4	4.9	5.4
K_2O	1.15	1.30	0.80	2.15	1.30	1.45
TiO_2	0.95	0.95	1.35	0.95	1.05	0.75
Total	99.40	99.45	99.75	99.60	97.95	99.00

HS7892 Elevation 4,760 ft., SW¼, NW¼, Sec. 8, T. 12 S., R. 19 E.; quartz-bearing andesite; Quartz-bearing Andesite Unit of Upper Clarno Formation.

HS7888 Elevation 4,300 ft., SE¼, NE¼, Sec. 8, T. 12 S., R. 19 E.; porphyritic pyroxene andesite; Pyroxene Andesite Unit of Upper Clarno Formation.

HS7861 Elevation 3,680 ft., NW¼, NE¼, Sec. 1, T. 12 S., R. 19 E.; porphyritic pyroxene andesite; Heflin Creek Member of Lower Clarno Formation.

HS78327 Elevation 3,720 ft., NW¼, SW¼, Sec. 3, T. 11 S., R. 19 E.; quartz-bearing andesite; Quartz-bearing Andesite Unit of Upper Clarno Formation.

HS78321 Elevation 4,200 ft., SE¼, NW¼, Sec. 6, T. 12 S., R. 19 E.; glassy andesite dike.

HS7887 Elevation 4,200 ft., NE¼, NE¼, Sec. 17, T. 12 S., R. 19 E.; aphanitic dacite plug.

Appendix B. SiO_2 and Al_2O_3 Variation Diagrams of Selected Clarno Rocks. (Points plotted are from analyses tabulated in Appendix A.)
Source of analyses:
× - Huggins (1978)
◦ - Barnes (1978)
+ - this study

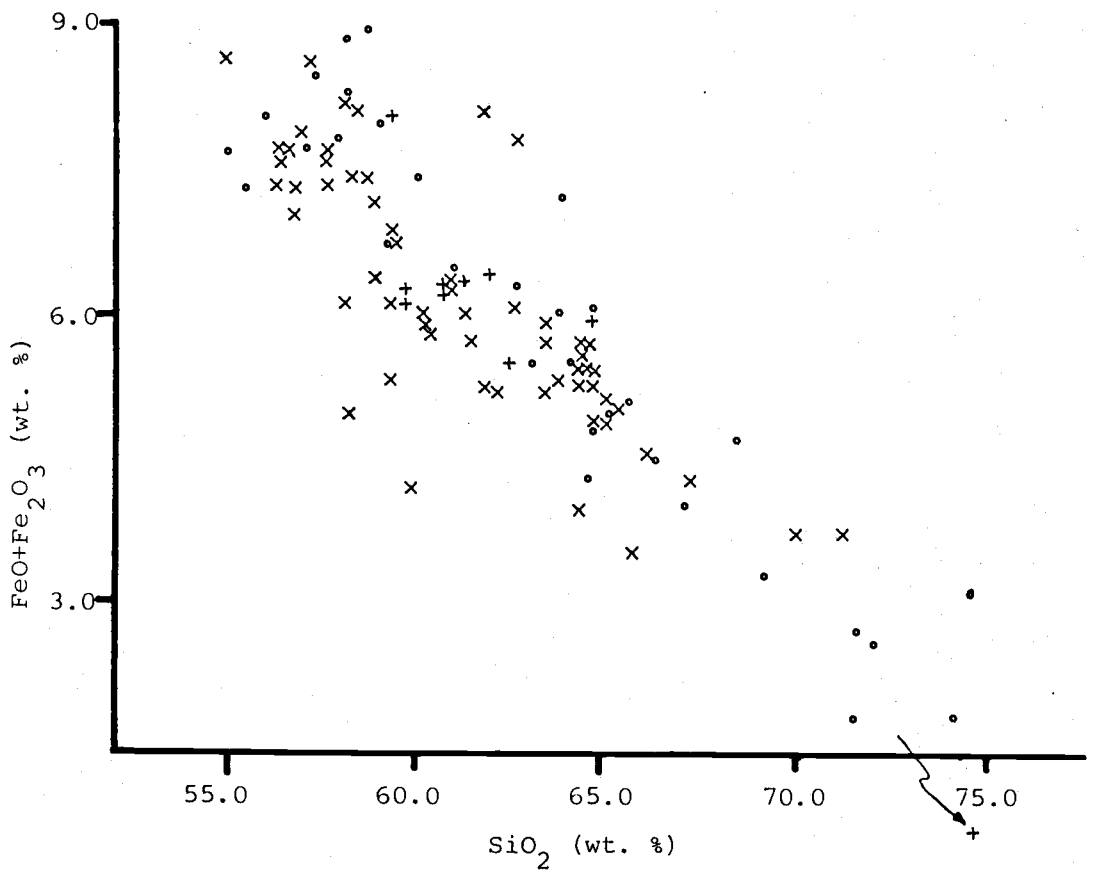

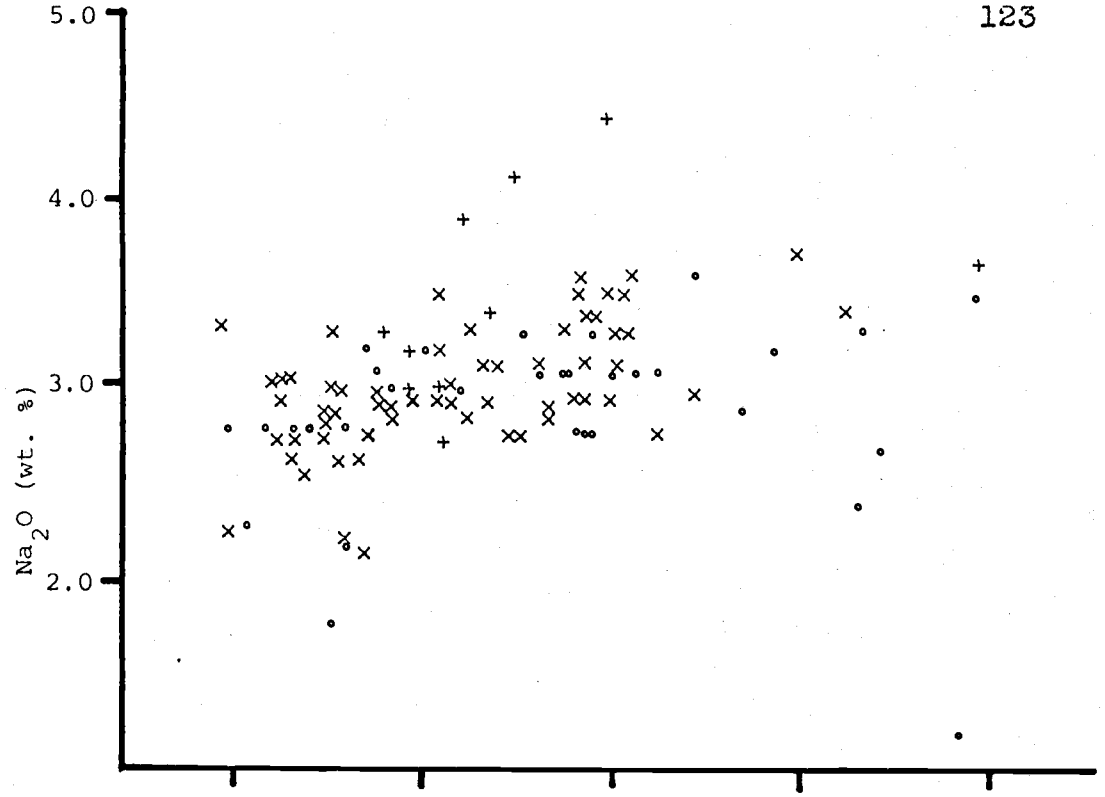
5.0
4.0
3.0
2.0
Na_2O (wt. %)

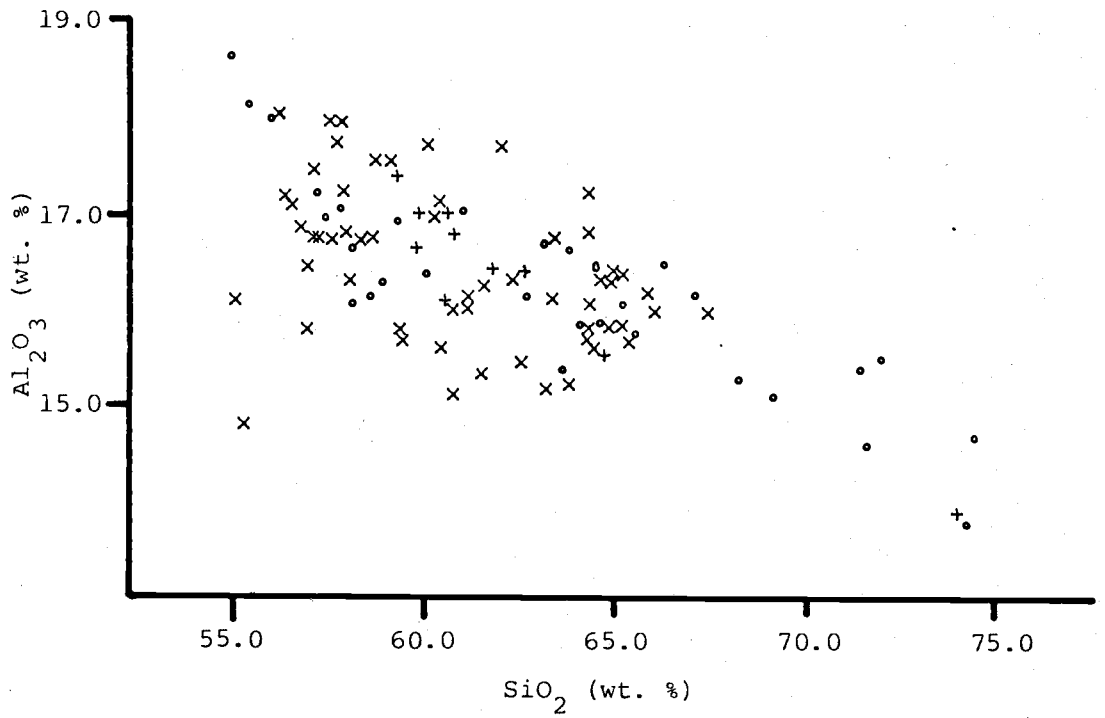
19.0
17.0
15.0
Al_2O_3 (wt. %)
55.0
60.0
65.0
70.0
75.0
SiO_2 (wt. %)

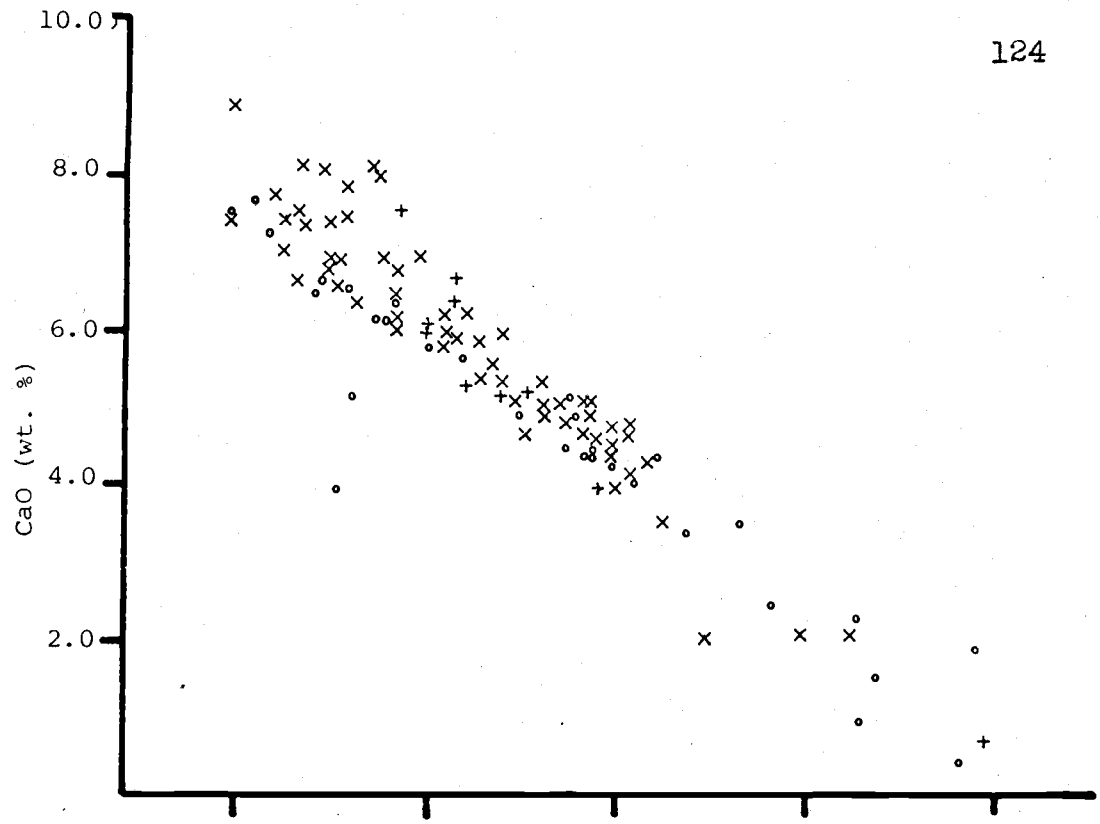
10.0
8.0
6.0
4.0
2.0
CaO (wt. %)

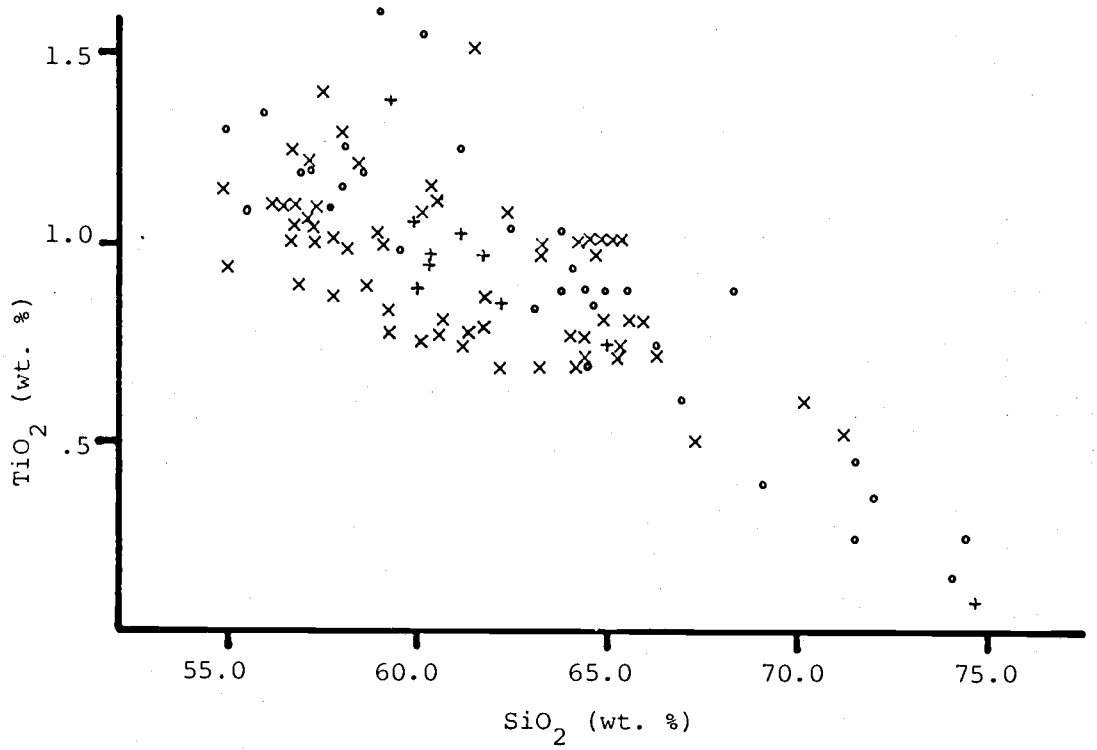
1.5
1.0
.5
TiO2 (wt. %)
55.0
60.0
65.0
70.0
75.0
SiO2 (wt. %)

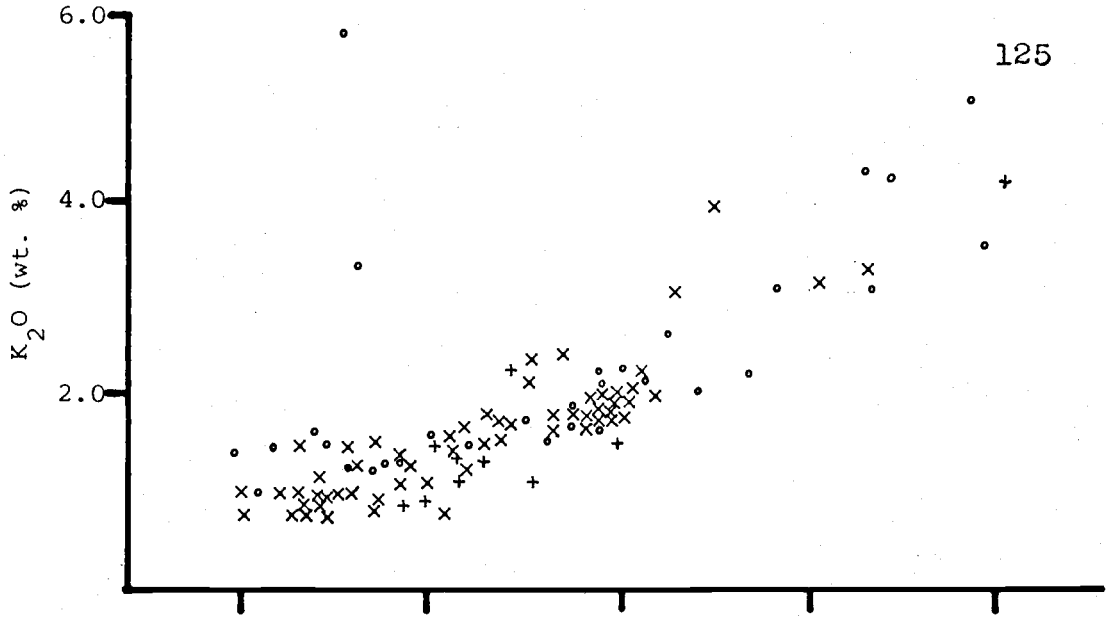
6.0
4.0
2.0
K_2O (wt. %)

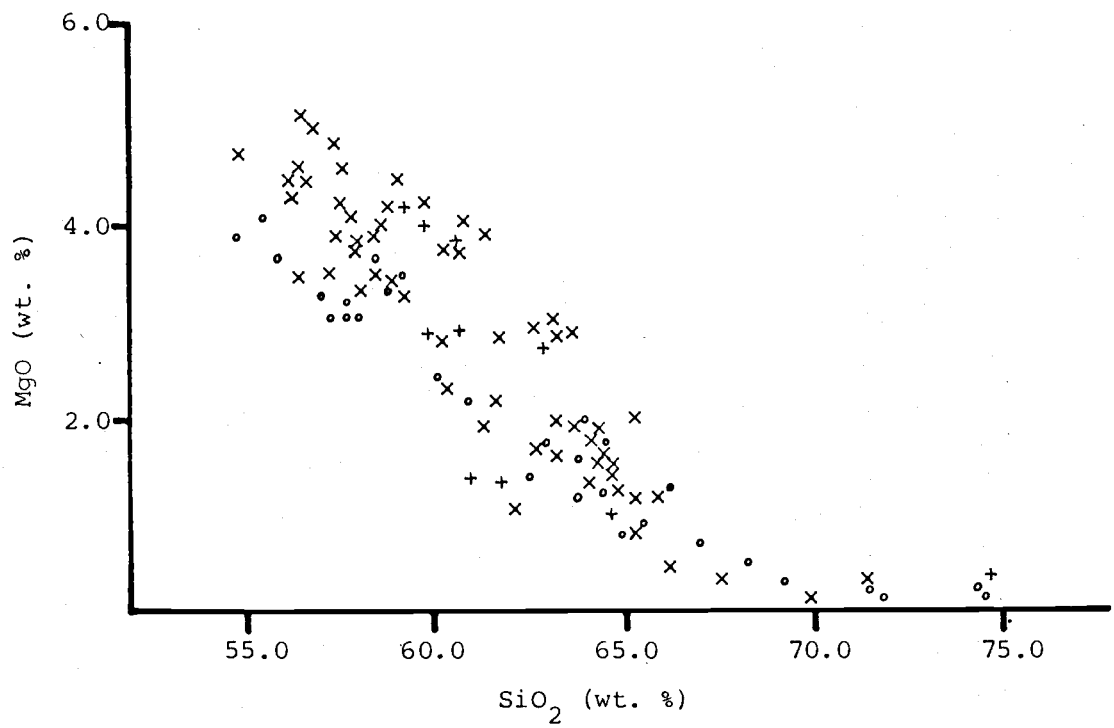
6.0
4.0
2.0
MgO (wt. %)
55.0
60.0
65.0
70.0
75.0
SiO_2 (wt. %)

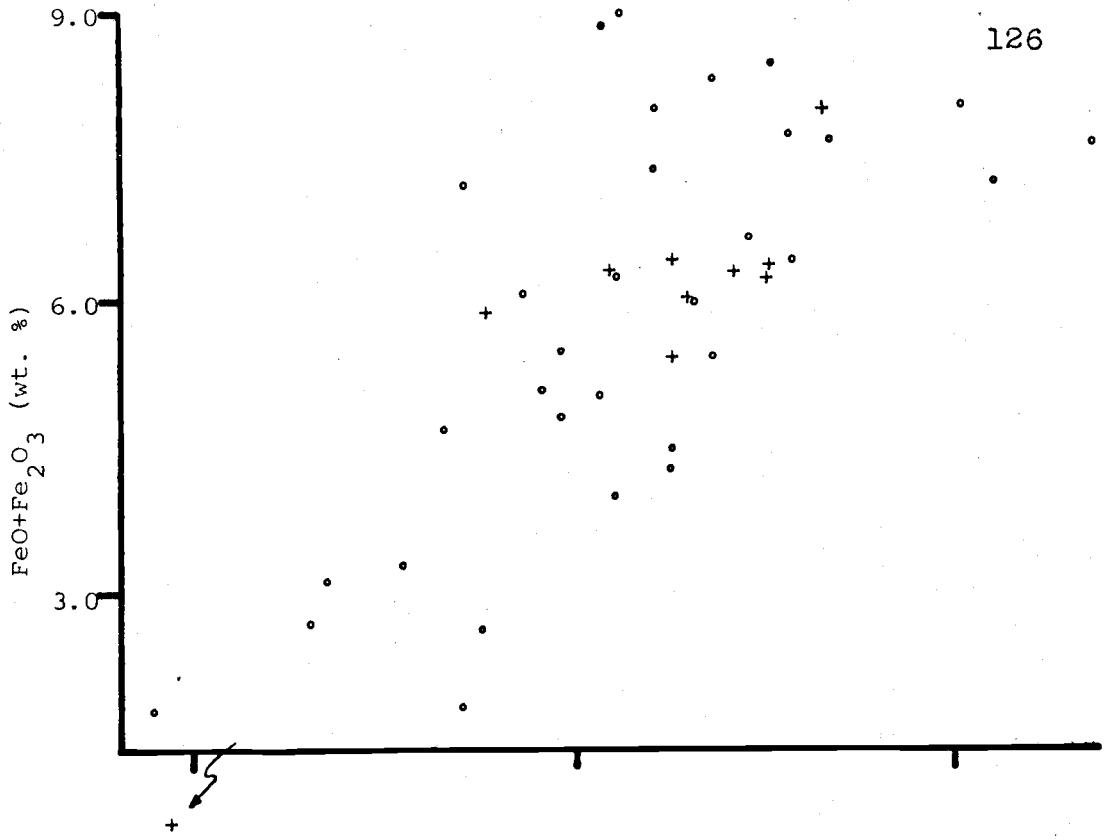
9.0
6.0
3.0
FeO+Fe2O3 (wt. %)

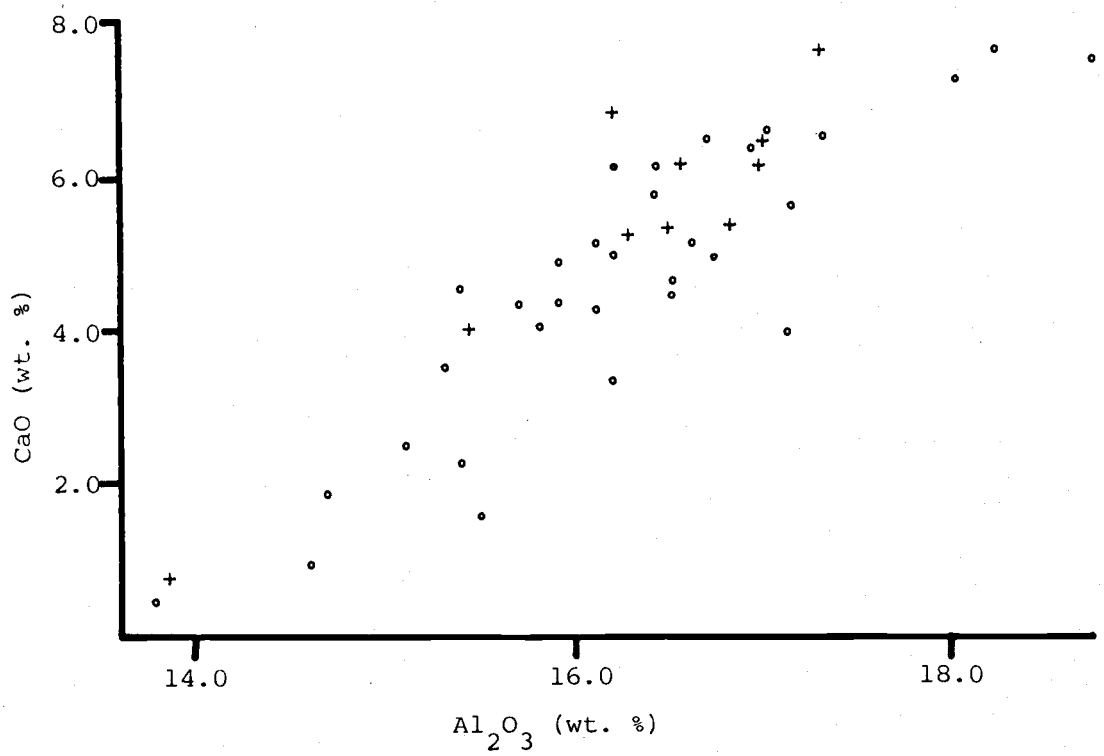
8.0
6.0
4.0
2.0
CaO (wt. %)
14.0
16.0
18.0
Al2O3 (wt. %)

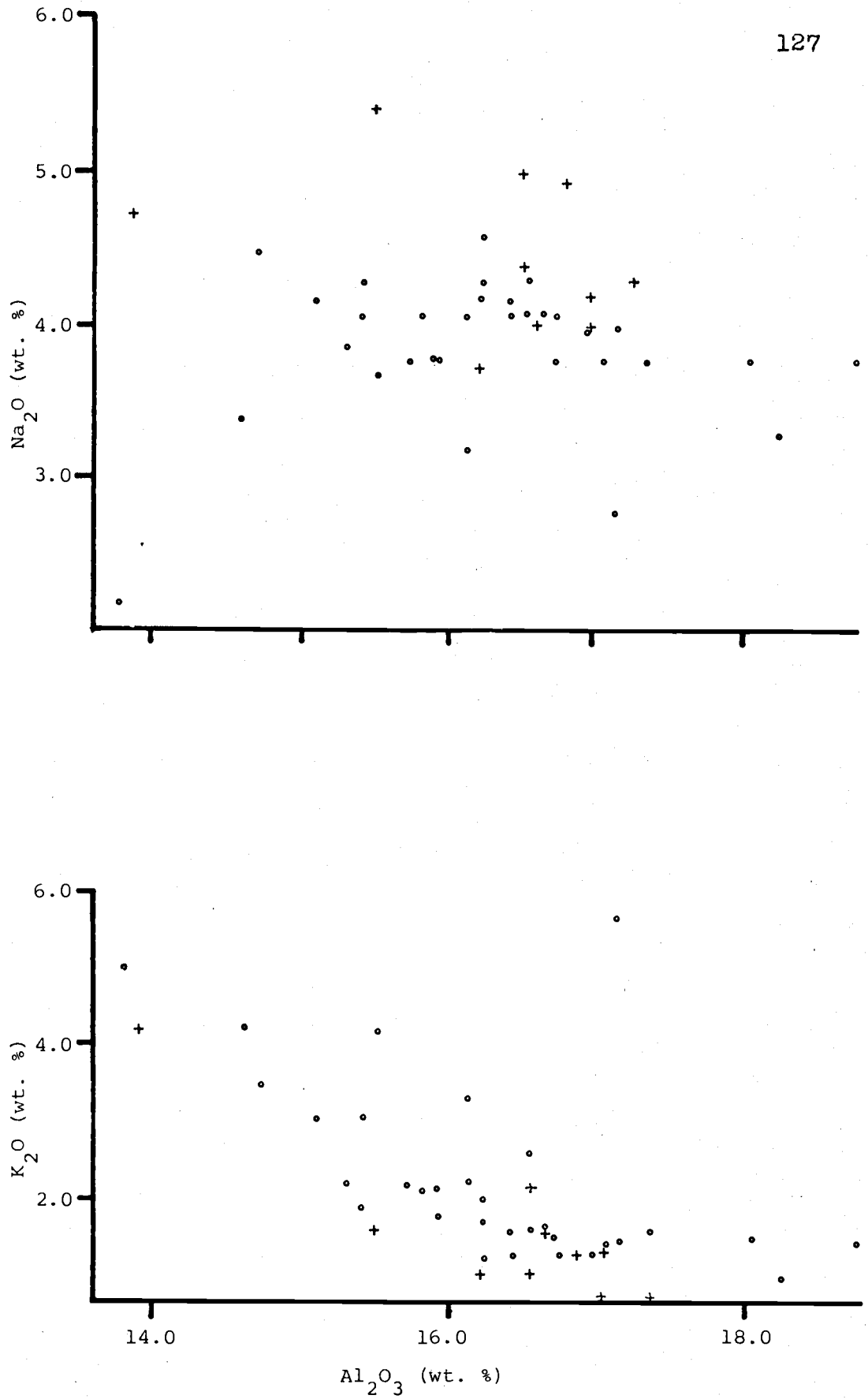
6.0
5.0
4.0
3.0
Na_2O (wt. %)
6.0
4.0
2.0
K_2O (wt. %)
14.0
16.0
18.0
Al_2O_3 (wt. %)

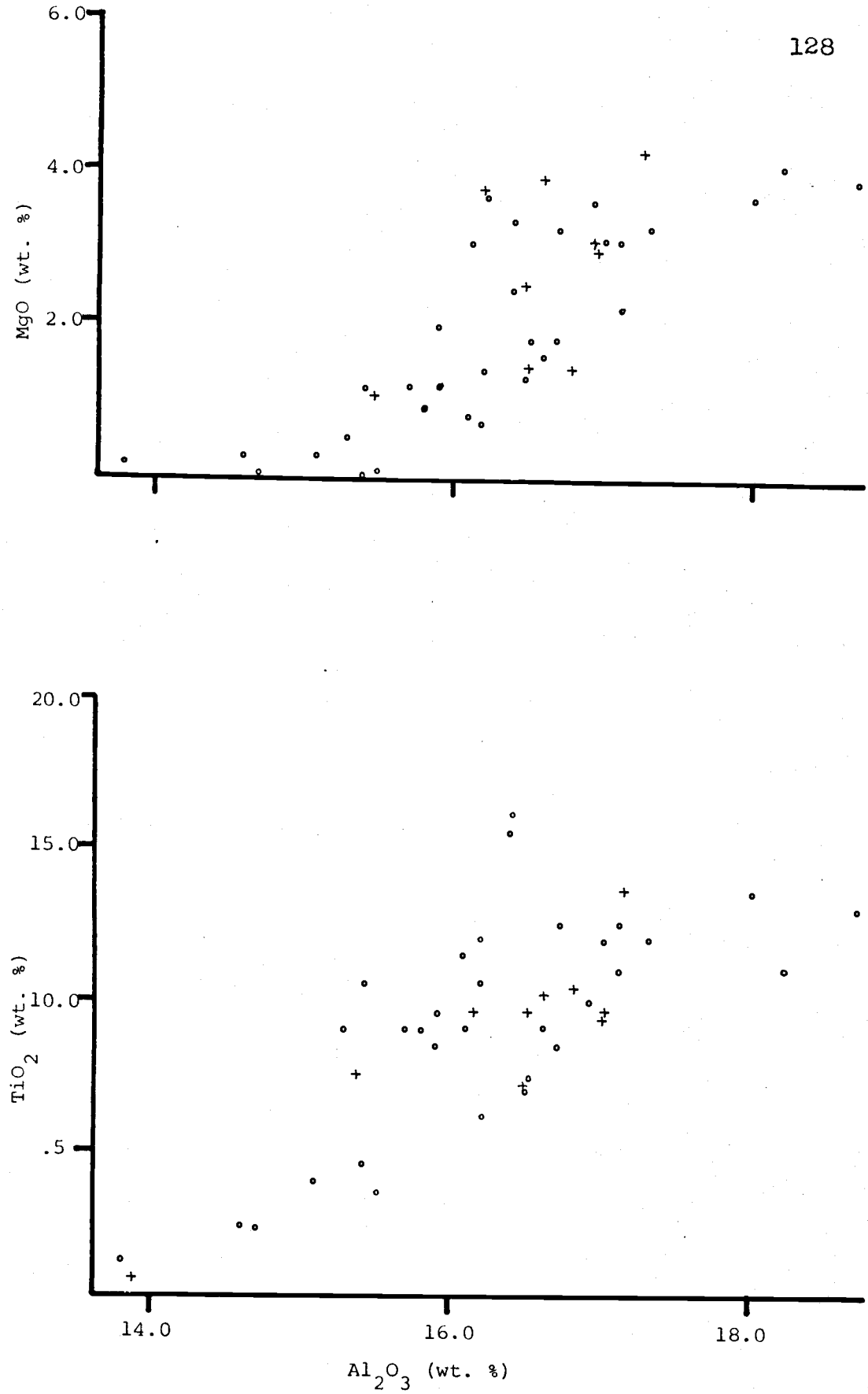
6.0
4.0
2.0
MgO (wt. %)
20.0
15.0
10.0
.5
TiO_2 (wt. %)
14.0
16.0
18.0
Al_2O_3 (wt. %)